International Journal of Solids and Structures 47 (2010) 786–800

Contents lists available at ScienceDirect

International Journal of Solids and Structures

journal homepage: www.elsevier.com/locate/ijsolstr

On finite strain micromorphic elastoplasticity

Richard A. Regueiro *

Department of Civil, Environmental, and Architectural Engineering, University of Colorado at Boulder, USA

ARTICLE INFO

Article history:
Received 14 December 2008
Received in revised form 8 November 2009
Available online 22 November 2009

Keywords:
Micromorphic elastoplasticity
Multiplicative decomposition
Finite strain

ABSTRACT

In the micromorphic continuum theory of Eringen, it was proposed that microstructure of materials could be represented in a continuum framework using a micro-deformation tensor governing micro-element deformation, in addition to the deformation gradient governing macro-element deformation. The paper formulates finite strain micromorphic elastoplasticity based on micromorphic continuum mechanics in the sense of Eringen. Multiplicative decomposition into elastic and plastic parts of the deformation gradient and micro-deformation are assumed, and the Clausius–Duhem inequality is formulated in the intermediate configuration $\overline{\mathscr{B}}$ to analyze what stresses, elastic deformation measures, and plastic deformation rates are used/defined in the constitutive equations. The resulting forms of plastic and internal state variable evolution equations can be viewed as phenomenological at their various scales (i.e., micro-continuum and macro-continuum). The phenomenology of inelastic mechanical material response at the various scales can be different, but for demonstration purposes, J_2 flow plasticity is assumed for each of three levels of plastic evolution equations identified, with different stress, internal state variables, and material parameters. All evolution equations and a semi-implicit time integration scheme are formulated in the intermediate configuration for future coupled Lagrangian finite element implementation. A simpler two-dimensional model for anti-plane shear kinematics is formulated to demonstrate more clearly how such model equations simplify for future finite element implementation.

1. Introduction

There currently is great interest in accounting for underlying microstructural response at the grain/particle/fiber scale on the overall continuum mechanical behavior of heterogeneous materials—such as polycrystalline metals, ceramics, concrete, masonry, geomaterials (soils and rocks), asphalt, bone—in terms of predicting their damage, fracture nucleation, and localized deformation. Much research has been done on traditional macro-continuum inelastic constitutive modeling such that a wide range of books are available to reference (Hill, 1950; Desai and Siriwardane, 1984; Lubliner, 1990; Maugin, 1992; Simo and Hughes, 1998; Simo, 1998; Nemat-Nasser, 2004). Likewise, research has been done and is ongoing on simulating directly the inelastic microstructural mechanical response—at the grain/particle/fiber scale—and reported in the literature (e.g., for polycrystalline metals (Vogler and Clayton, 2008), ceramics (Maiti et al., 2005; Molinari and Warner, 2006; Sadowski et al., 2007), concrete (Caballero et al., 2006), masonry (Formica et al., 2002), geomaterials (soils (Nezami et al., 2007) and rocks (Morris et al., 2006)), asphalt (Birgisson et al., 2004; Dai et al., 2005), bone (Chevalier et al., 2007; Lee et al., 2007)). One of the current research challenges, however, is how to bridge these length scales, from grain/particle/fiber scale (sometimes called the 'meso'-scale) to the macro-continuum scale of the engineering application, without losing salient kinematic structure and micro-stresses. The finite strain micromorphic elastoplasticity model framework presented in the paper is meant to bridge the mechanics between the grain/particle/fiber and macro-scales: to do so not only in a hierarchical information-passing (homogenization) multi-scale fashion, but also for concurrent multiscale modeling (Fish, 2006). Concurrent multiscale modeling, in our case, would involve retaining the grain/particle/fiber scale resolution in spatial regions of interest—for instance where damage/micro-cracking nucleates or at the interface between contacting materials—while transitioning to a 'far'-field macro-scale continuum representation via a micromorphic continuum region (Fig. 1). The additional degrees of freedom (dofs) and constitutive richness of the micromorphic continuum mechanics and plasticity equations provide a more plausible transition than standard macro-continuum mechanics. We note that these additional dofs are still fewer than if a micromechanical finite element simulation is attempted for the whole spatial domain, which is the argument in favor of concurrent multiscale models: that is, using high-fidelity materials modeling where needed (e.g., at a crack tip or large shear deformation interface, Fig. 1), and less fidelity where not needed.

The paper proposes a phenomenological bridging-scale constitutive modeling framework in the context of finite strain micromorphic elastoplasticity based on a multiplicative decomposition

* Fax: +1 303 492 7317.
E-mail address: regueiro@colorado.edu

0020-7683/$ - see front matter © 2009 Elsevier Ltd. All rights reserved.
doi:10.1016/j.ijsolstr.2009.11.006

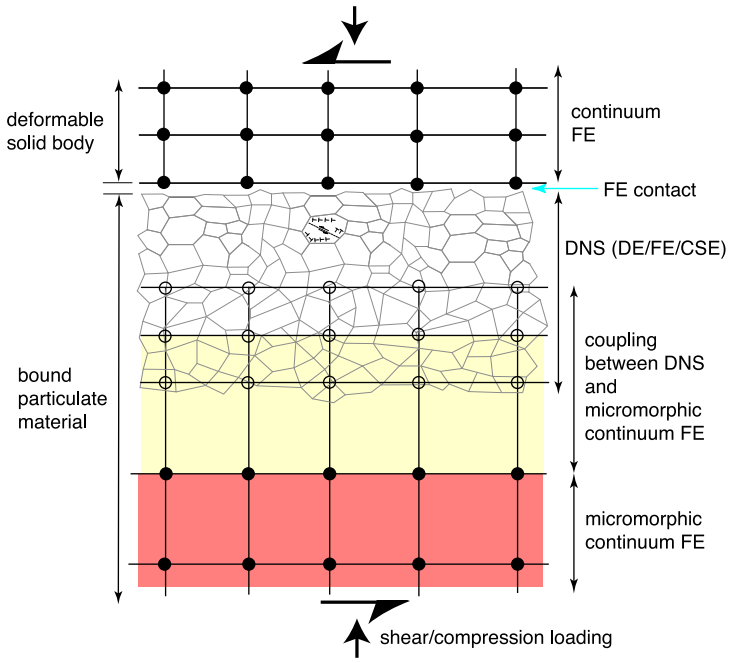

Fig. 1. Illustration of concurrent computational multi-scale modeling approach in the contact interface region between a bound particulate material and deformable solid body. The grains (binder matrix not shown) of the micro-structure are 'meshed' directly (direct numerical simulation (DNS)) using discrete elements (DEs) and/or finite elements (FEs) with cohesive surface elements (CSEs) at their interfaces. The open circles denote micromorphic continuum FE nodes that have prescribed degrees of freedom (dofs) $\bar{\boldsymbol{D}}$ based on the underlying grain-scale response, while the solid circles denote micromorphic continuum FE nodes that have free dofs $\boldsymbol{D}$ governed by the micromorphic continuum elasto-plastic model.

of the deformation gradient $\boldsymbol{F}$ and micro-deformation tensor $\boldsymbol{\chi}$ into elastic and plastic parts. In addition to the three translational displacement vector $\boldsymbol{u}$ degrees of freedom (dofs), there are nine dofs associated with the unsymmetric micro-deformation tensor $\boldsymbol{\chi}$ (micro-rotation, micro-stretch, and micro-shear). We leave the formulation general in terms of $\boldsymbol{\chi}$, which can be further simplified depending on the material and associated constitutive assumptions (see Forest and Sievert (2003, 2006)). The Clausius–Duhem inequality formulated in the intermediate configuration yields the mathematical form of three levels of plastic evolutions equations in either (1) Mandel stress form (Mandel et al., 1974), or (2) an alternate 'metric' form. For demonstration of the micromorphic elastoplasticity modeling framework, J_2 flow plasticity and linear isotropic elasticity are assumed. A semi-implicit time integration scheme is also presented for implementation in a coupled Lagrangian finite element code in the future. A two-dimensional strict anti-plane shear model is presented to discuss a simpler model with future finite element implementation.

The formulation presented in the paper differs from other works on finite strain micromorphic elastoplasticity that consider a multiplicative decomposition into elastic and plastic parts (Sansour, 1998; Forest and Sievert, 2003, 2006) and those that do not (Lee and Chen, 2003; Vernerey et al., 2007).

Sansour (1998) considered a finite strain Cosserat and micromorphic plastic continuum, redefining the micromorphic strain measures (see (119) in Appendix B) to be invariant with respect to rigid rotations only, not also translations. Sansour did not extend his formulation to include details on a finite strain micromorphic elastoplasticity constitutive model formulation, as this paper does. Sansour proposed to arrive at the higher-order macro-continuum by integrally averaging micro-continuum plasticity behavior using computation. Such an approach is similar to computational homogenization, as proposed by Forest and Sievert (2006) to estimate material parameters for generalized continuum plasticity models. On a side note, one advantage to the micromorphic continuum approach by Eringen and Suhubi (1964) is that the integral-averaging of certain stresses, body forces, and micro-inertia terms is already part of the formulation. This will become especially useful when computationally homogenizing underlying microstructural mechanical response (e.g., provided by a microstructural finite element or discrete element simulation) in regions of interest, such as overlapping between micromorphic continuum and grain/particle/fiber representations for a concurrent multiscale modeling approach (Fig. 1).

Forest and Sievert (2003, 2006) established a hierarchy of elasto-plastic models for generalized continua, including Cosserat, higher grade, and micromorphic at small and finite strain. Specifically with regard to micromorphic finite strain theory, Forest and Sievert (2003) follows the approach of Germain (1973), which leads to different stress power terms in the balance of energy and, in turn, Clausius–Duhem inequality than presented by Eringen (1999). Also, the invariant elastic deformation measures do not match the sets (39) and (119) proposed by Eringen (1999). Upon analyzing the change in square of micro-element arc-lengths $(ds')^2 - \left(d\bar{S}'\right)^2$ between current $\mathscr{B}$ and intermediate configurations $\overline{\mathscr{B}}$ (cf. Appendix A), then either set (39) or (119) is unique. Forest and Sievert (2003, 2006) proposed to use a mix of the two sets, i.e. $(39)_1$, $(119)_2$, and $(119)_3$, in their Helmholtz free energy function. When analyzing $(ds')^2 - \left(d\bar{S}'\right)^2$, they would also need $(119)_1$ as a fourth elastic deformation measure. As Eringen proposed, however, it is more straightforward to use either set (39) or (119) when representing elastic deformation. The paper analyzes the use of both sets. Mandel stress tensors are identified in Forest and Sievert (2003, 2006) to use in the plastic evolution equations. This paper presents additional Mandel stresses and considers also an alternate 'metric'-form oftentimes used in finite deformation elastoplasticity modeling.

Vernerey et al. (2007) treated micromorphic plasticity modeling similar to Germain (1973) and Mindlin (1964), which leads to

different stress power terms and balance equations than in Eringen (1999). The resulting plasticity model form is thus similar to Forest and Sievert (2003), although does not use a multiplicative decomposition and thus does not assume the existence of an intermediate configuration. An extension presented by Vernerey et al. is to consider multiple scale micromorphic kinematics, stresses, and balance equations, where the number of scales is a choice made by the constitutive modeler. A multiple scale averaging procedure is introduced to determine material parameters at the higher scales based on lower scale response.

In general, in terms of a multiplicative decomposition of the deformation gradient and micro-deformation, as compared to recent formulations of finite strain micromorphic elastoplasticity reported in the literature (just reviewed in preceding paragraphs), we view our approach to be more in line with the original concept and formulation presented by Eringen and Suhubi (1964, 1999), which provide a clear link between micro-element and macro-element deformation, balance equations, and stresses. Thus, we believe our formulation and resulting elastoplasticity model framework is more general than what has been presented previously. The paper by Lee and Chen (2003) also follows closely Eringen's micromorphic kinematics and balance laws, but does not treat multiplicative decomposition kinematics and subsequent constitutive model form in the intermediate configuration, as this paper does. We demonstrate the formulation for three levels of J_2 plasticity and linear isotropic elasticity, and numerical time integration by a semi-implicit scheme, as well as restriction to strict anti-plane shear kinematics.

Index notation will be used throughout so as to be as clear as possible with regard to details of the formulation. Some symbolic/direct notation is also given, such that $(\boldsymbol{ab})_{ik} = a_{ij}b^{j}_{\cdot k}$, $(\boldsymbol{a}\otimes\boldsymbol{b})_{ijkl} = a_{ij}b_{kl}$, $(\boldsymbol{a}\odot\boldsymbol{c})^{ij}_{\cdot\cdot k} = a^{im}c^{j}_{\cdot mk}$. Boldface denotes a tensor or vector, where its index notation has been given uniformly throughout the paper. Generally, variables in uppercase letters and no overbar live in the reference configuration $\mathscr{B}_0$ (such as the reference differential volume dV), variables in lowercase live in the current configuration $\mathscr{B}$ (such as the current differential volume dv), and variables in uppercase with overbar live in the intermediate configuration $\overline{\mathscr{B}}$ (such as the intermediate differential volume $d\overline{V}$). The same applies to their indices, such that a differential line segment in the current configuration dx^i (contravariant component of $d\boldsymbol{x} = dx^i\boldsymbol{g}_i$) is related to a differential line segment in the reference configuration dX^I through the deformation gradient: $dx^i = F^i_{\cdot I}dX^I$ (Einstein's summation convention assumed (see, Eringen, 1962; Holzapfel, 2000)). In addition, the multiplicative decomposition of the deformation gradient is written as $F^i_{\cdot I} = F^{ei}_{\quad\bar{I}}F^{p\bar{I}}_{\quad\cdot I}(\boldsymbol{F} = \boldsymbol{F}^e\boldsymbol{F}^p)$, where superscripts e and p denote elastic and plastic parts, respectively. Subscripts $(\bullet)_{,i}$, $(\bullet)_{,\bar{I}}$ and $(\bullet)_{,I}$ imply covariant differentiation in the reference, intermediate, and current configurations, respectively, whereas $\partial_i(\bullet) = \partial(\bullet)/\partial x^i$ denotes a partial derivative, in this case in $\mathscr{B}$. With an eye toward eventual continuum finite element implementation of a resulting micromorphic elastoplasticity model, the reference, intermediate, and current configurations will be assumed Cartesian in the future. A superscript prime symbol $(\bullet)'$ denotes a variable associated with the micro-element (see Section 2 on kinematics). Superposed dot $\dot{(\square)} = D(\square)/Dt$ denotes material time derivative.

An outline of the remainder of the paper is as follows: Section 2 describes micromorphic kinematics based on multiplicative decompositions of $\boldsymbol{F}$ and $\boldsymbol{\chi}$ into elastic e and plastic p parts; Section 3 the balance equations; Section 4 the Clausius–Duhem inequality; Section 5 constitutive form and reduced dissipation inequality; Section 6 form of plastic evolution equations; Section 7 constitutive equations for linear isotropic elasticity and J_2 plasticity; Section 8 semi-implicit time integration; Section 9 anti-plane shear model; and Section 10 conclusions.

2. Micromorphic kinematics

Fig. 2 illustrates the mapping of the macro-element and micro-element in the reference configuration to the current configuration through the deformation gradient $\boldsymbol{F}$ and micro-deformation tensor $\boldsymbol{\chi}$. The macro-element continuum point is denoted by $P(\boldsymbol{X},\boldsymbol{\Xi})$ and $p(\boldsymbol{x},\boldsymbol{\xi},t)$ in the reference and current configurations, respectively, with centroid C and c. The micro-element continuum point centroid is denoted by C' and c' in the reference and current configurations, respectively. The micro-element is denoted by an assembly of particles, but in general represents a grain/particle/fiber microstructural sub-volume of the heterogeneous material. The relative position vector of the micro-element centroid with respect to the macro-element centroid is denoted by $\boldsymbol{\Xi}$ and $\boldsymbol{\xi}(\boldsymbol{X},\boldsymbol{\Xi},t)$ in the reference and current configurations, respectively, such that the micro-element centroid position vectors are written as (Fig. 2) (Eringen, 1999) (in terms of contravariant components)

$$X'^K = X^K + \Xi^K, \quad x'^k = x^k(\boldsymbol{X},t) + \xi^k(\boldsymbol{X},\boldsymbol{\Xi},t) \tag{1}$$

Eringen and Suhubi (1964) assumed that for sufficiently small lengths $\|\boldsymbol{\Xi}\| \ll 1$ ($\|\bullet\|$ is the L_2 norm), $\boldsymbol{\xi}$ is linearly related to $\boldsymbol{\Xi}$ through the micro-deformation tensor $\boldsymbol{\chi}$, such that

$$\xi^k(\boldsymbol{X},\boldsymbol{\Xi},t) = \chi^k_{\cdot K}(\boldsymbol{X},t)\Xi^K \tag{2}$$

where then the spatial position vector of the micro-element centroid is written as

$$x'^k = x^k(\boldsymbol{X},t) + \chi^k_{\cdot K}(\boldsymbol{X},t)\Xi^K \tag{3}$$

This is equivalent to assuming an affine, or homogeneous, deformation of the macro-element differential volume dV (but *not* the body $\mathscr{B}$; i.e., the continuum body $\mathscr{B}$ is expected to experience heterogeneous deformation because of $\boldsymbol{\chi}$, even if boundary conditions (BCs) are uniform). It also simplifies considerably the formulation of the micromorphic continuum balance equations as presented in Eringen and Suhubi (1964) and Eringen (1999). This micro-deformation $\boldsymbol{\chi}$ is analogous to the small strain micro-deformation tensor $\boldsymbol{\psi}$ in Mindlin (1964), physically described in his Fig. 1. Eringen (1968) also provides a physical interpretation of $\boldsymbol{\chi}$ generally, but then simplies for the micropolar case. For example, $\boldsymbol{\chi}$ can be interpreted

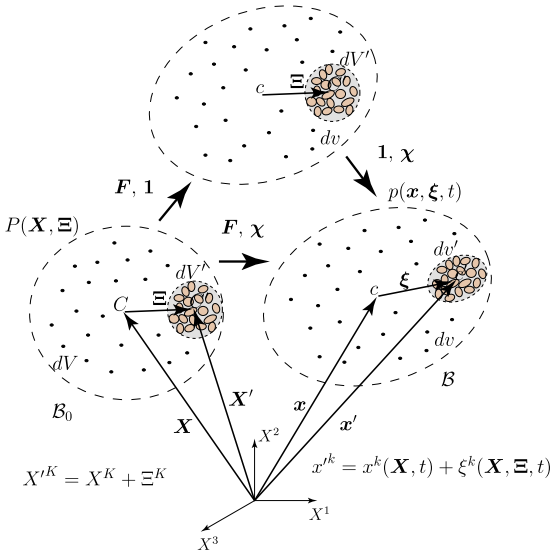

Fig. 2. Map from reference $\mathscr{B}_0$ to current configuration $\mathscr{B}$ accounting for relative position $\boldsymbol{\Xi}$, $\boldsymbol{\xi}$ of micro-element centroid C', c' with respect to centroid of macro-element C, c. $\boldsymbol{F}$ and $\boldsymbol{\chi}$ can load and unload independently (although coupled through constitutive equations and balance equations), and thus the additional current configuration is shown.

as calculated from a micro-displacement gradient tensor $\boldsymbol{\Phi}$ as $\boldsymbol{\chi} = \mathbf{1} + \boldsymbol{\Phi}$, where $\boldsymbol{\Phi}$ is not actually calculated from a micro-displacement vector $\boldsymbol{u}'$, but a $\boldsymbol{u}'$ can be calculated once $\boldsymbol{\chi}$ is known. For finite element implementation, $\boldsymbol{\Phi}$ will be interpolated at the nodes, providing an additional nine dofs because it is unsymmetric. The micro-element spatial velocity vector (holding $\boldsymbol{X}$ and $\boldsymbol{\Xi}$ fixed) is then written as

$$v'^k = v^k + \dot{\xi}^k = v^k + v^k_{,l}\xi^l \tag{4}$$

where v^k is the macro-element spatial velocity vector, $v^k_{,l} = \dot{\chi}^k_{,K}(\chi^{-1})^K_{,l}$ ($\boldsymbol{v} = \dot{\boldsymbol{\chi}}\boldsymbol{\chi}^{-1}$) the micro-gyration tensor, similar in form to the velocity gradient $v^k_{,l} = \dot{F}^k_{,K}(F^{-1})^K_{,l}$ ($\boldsymbol{\ell} = \dot{\boldsymbol{F}}\boldsymbol{F}^{-1}$).

Now we take the partial spatial derivative of (3) with respect to the reference micro-element position vector X'^K, to arrive at an expression for the micro-element deformation gradient $F'^k_{,K}$ as (see Appendix C)

$$F'^k_{,K} = F^k_{,K}(\boldsymbol{X},t) + \frac{\partial \chi^k_{,L}(\boldsymbol{X},t)}{\partial X^K}\Xi^L + \left(\chi^k_{,A}(\boldsymbol{X},t) - F^k_{,A}(\boldsymbol{X},t) - \frac{\partial \chi^k_{,M}(\boldsymbol{X},t)}{\partial X^A}\Xi^M\right)\frac{\partial \Xi^A}{\partial X^K} \tag{5}$$

where the deformation gradient of the macro-element is $F^k_{,K} = \partial x^k(\boldsymbol{X},t)/\partial X^K$. The micro-element deformation gradient $F'^k_{,K}$ maps micro-element differential line segments $dx'^k = F'^k_{,K}dX'^K$ and volumes $dv' = J'dV'$, where $J' = \det \boldsymbol{F}'$ is the micro-element Jacobian of deformation. This is presented for generality of mapping stresses between $\mathscr{B}_0$ and $\mathscr{B}$, $\mathscr{B}_0$ and $\overline{\mathscr{B}}$, $\overline{\mathscr{B}}$ and $\mathscr{B}$, as shown starting in (22), but will not be used explicitly in the constitutive equations in Section 7.

We now assume a multiplicative decomposition of the deformation gradient (Lee, 1969) and micro-deformation (Sansour, 1998; Forest and Sievert, 2003, 2006) (Fig. 3), such that

$$\boldsymbol{F} = \boldsymbol{F}^e\boldsymbol{F}^p, \quad \boldsymbol{\chi} = \boldsymbol{\chi}^e\boldsymbol{\chi}^p \tag{6}$$
$$F^k_{,K} = F^{ek}_{,\bar{k}}F^{p\bar{k}}_{,K}, \quad \chi^k_{,K} = \chi^{ek}_{,\bar{k}}\chi^{p\bar{k}}_{,K}$$

Given the multiplicative decompositions of $\boldsymbol{F}$ and $\boldsymbol{\chi}$, the velocity gradient and micro-gyration tensors can be expressed as

$$\boldsymbol{\ell} = \dot{\boldsymbol{F}}^e\boldsymbol{F}^{e-1} + \boldsymbol{F}^e\bar{\boldsymbol{L}}^p\boldsymbol{F}^{e-1} = \boldsymbol{\ell}^e + \boldsymbol{\ell}^p \tag{7}$$
$$v^l_{,k} = \dot{F}^{el}_{,\bar{A}}(F^{e-1})^{\bar{A}}_{,k} + F^{el}_{,\bar{B}}\bar{L}^{p\bar{B}}_{,\bar{C}}(F^{e-1})^{\bar{C}}_{,k} = \ell^{el}_{,k} + \ell^{pl}_{,k}$$
$$\bar{L}^{p\bar{B}}_{,\bar{C}} = \dot{F}^{p\bar{B}}_{,B}(F^{p-1})^{B}_{,\bar{C}}$$
$$\boldsymbol{v} = \dot{\boldsymbol{\chi}}^e\boldsymbol{\chi}^{e-1} + \boldsymbol{\chi}^e\bar{\boldsymbol{L}}^{\chi,p}\boldsymbol{\chi}^{e-1} = \boldsymbol{v}^e + \boldsymbol{v}^p \tag{8}$$
$$v^l_{,k} = \dot{\chi}^{el}_{,\bar{A}}(\chi^{e-1})^{\bar{A}}_{,k} + \chi^{el}_{,\bar{B}}\bar{L}^{\chi,p\bar{B}}_{,\bar{C}}(\chi^{e-1})^{\bar{C}}_{,k} = v^{el}_{,k} + v^{pl}_{,k}$$
$$\bar{L}^{\chi,p\bar{B}}_{,\bar{C}} = \dot{\chi}^{p\bar{B}}_{,B}(\chi^{p-1})^{B}_{,\bar{C}}$$

In the next section, the Clausius–Duhem inequality requires the covariant derivative of the micro-gyration tensor, which will be split into elastic and plastic parts based on (8). Thus, it is written as

$$\boldsymbol{\nabla}\boldsymbol{v} = \boldsymbol{\nabla}\boldsymbol{v}^e + \boldsymbol{\nabla}\boldsymbol{v}^p \tag{9}$$
$$v^l_{,m,k} = v^{el}_{,m,k} + v^{pl}_{,m,k}$$
$$v^{el}_{,m,k} = \dot{\chi}^{el}_{,\bar{A},k}(\chi^{e-1})^{\bar{A}}_{,m} - v^{el}_{,n}\chi^{en}_{,\bar{D},k}(\chi^{e-1})^{\bar{D}}_{,m} \tag{10}$$
$$v^{pl}_{,m,k} = \left(\chi^{el}_{,\bar{C},k}\dot{\chi}^{p\bar{C}}_{,A} + \chi^{el}_{,\bar{E}}\dot{\chi}^{p\bar{E}}_{,A,k} - \chi^{el}_{,\bar{F}}\bar{L}^{\chi,p\bar{F}}_{,\bar{G}}\chi^{p\bar{G}}_{,A,k}\right)(\chi^{-1})^{A}_{,m} - v^{pl}_{,a}\chi^{ea}_{,\bar{A},k}(\chi^{e-1})^{\bar{A}}_{,m} \tag{11}$$

The covariant derivative (i.e., the gradient) of the elastic microdeformation tensor $\boldsymbol{\nabla}\boldsymbol{\chi}^e$ is analogous to the small strain micro-deformation gradient $\mathscr{N}$ in Mindlin (1964), and its physical interpretation in Fig. 2 of Mindlin (1964). For example, $(\chi^e)^1_{1,2}$ is an elastic micro-shear gradient in the x_2-direction based on a micro-stretch in the x_1-direction. Furthermore, just as differential macro-element volumes map as

$$dv = JdV = J^eJ^pdV = J^ed\bar{V} \tag{12}$$

where $J^e = \det \boldsymbol{F}^e$ and $J^p = \det \boldsymbol{F}^p$, then micro-element differential volumes map as

$$dv' = J'dV' = J^{e\prime}J^{p\prime}dV' = J^{e\prime}d\bar{V}' \tag{13}$$

where $J^{e\prime} = \det \boldsymbol{F}^{e\prime}$ and $J^{p\prime} = \det \boldsymbol{F}^{p\prime}$. $\boldsymbol{F}^{e\prime}$ and $\boldsymbol{F}^{p\prime}$ have not been defined from (5), and are not required for formulating the final constitutive equations. Likewise, according to micro- and macro-element mass conservation, mass densities map as

$$\rho_0 = \rho J = \rho J^eJ^p = \bar{\rho}J^p \tag{14}$$
$$\rho'_0 = \rho' J' = \rho' J^{e\prime}J^{p\prime} = \bar{\rho}' J^{p\prime} \tag{15}$$

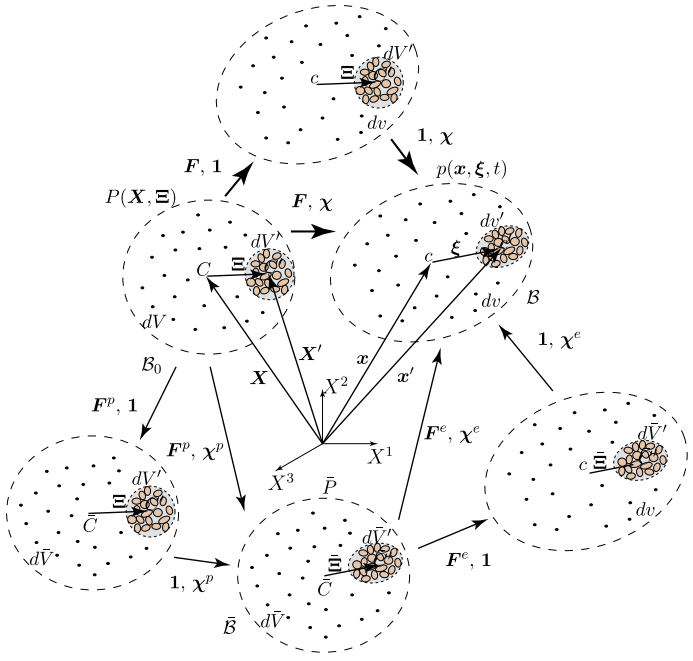

Fig. 3. Multiplicative decomposition of deformation gradient $\boldsymbol{F}$ and microdeformation tensor $\boldsymbol{\chi}$ into elastic and plastic parts, and the existence of an intermediate configuration $\overline{\mathscr{B}}$. Since $\boldsymbol{F}^e$, $\boldsymbol{F}^p$, $\boldsymbol{\chi}^e$, and $\boldsymbol{\chi}^p$ can load and unload independently (although coupled through constitutive equations and balance equations), additional configurations are shown. The constitutive equations and balance equations presented in the paper will govern these deformation processes, and so generality is preserved.

This last result was achieved by using a volume-average definition relating macro-element mass density to micro-element mass density as

$$\rho dv \overset{\text{def}}{=} \int_{dv} \rho' \, dv', \quad \rho_0 dV \overset{\text{def}}{=} \int_{dV} \rho'_0 \, dV', \quad \bar{\rho} d\overline{V} \overset{\text{def}}{=} \int_{d\overline{V}} \bar{\rho}' \, d\overline{V}' \tag{16}$$

This volume averaging approach by Eringen and Suhubi (1964) is used extensively in formulating the balance equations and Clausius–Duhem inequality.

3. Micromorphic balance equations and Clausius–Duhem inequality

Details regarding the formulation of micromorphic balance equations and the Clausius–Duhem inequality are given in Eringen and Suhubi (1964) and Eringen (1999) and thus are not repeated here. The equations are summarized over the current configuration $\mathscr{B}$ for balance of linear and first moment of momentum, balance of energy, and the Clausius–Duhem inequality, respectively, as

$$\sigma^{lk}_{,l} + \rho(f^k - a^k) = 0 \tag{17}$$

$$\sigma^{ml} - s^{ml} + m^{klm}_{,k} + \rho(\lambda^{lm} - \omega^{lm}) = 0 \tag{18}$$

$$s^{ml} dv \overset{\text{def}}{=} \int_{dv} \sigma'^{ml} \, dv', \quad m^{klm} n_k da \overset{\text{def}}{=} \int_{da} \sigma'^{kl} \xi^m n'_k \, da'$$

$$\rho \lambda^{lm} dv \overset{\text{def}}{=} \int_{dv} \rho' f'^l \xi^m \, dv', \quad \rho \omega^{lm} dv \overset{\text{def}}{=} \int_{dv} \rho' \ddot{\xi}^l \xi^m \, dv'$$

$$\rho \dot{e} = (s^{kl} - \sigma^{kl}) v_{lk} + \sigma^{kl} v_{lk} + m^{klm} v_{lm,k} + q^k_{,k} + \rho r \tag{19}$$

$$-\rho(\dot{\psi} + \eta\dot{\theta}) + \sigma^{kl}(v_{l,k} - v_{lk}) + s^{kl} v_{lk} + m^{klm} v_{lm,k} + \frac{1}{\theta} q^k \theta_{,k} \geqslant 0 \tag{20}$$

where σ^{lk} are contravariant components of the unsymmetric Cauchy stress, ρ is the mass density, f^k is the body force vector per unit mass, f'^l is the body force vector per unit mass over the micro-element, a^k is the acceleration, s^{ml} are the contravariant components of the symmetric micro-stress, m^{klm} are the contravariant components of the higher order couple stress, λ^{lm} the body force couple per unit mass, ω^{lm} the micro-spin inertia per unit mass, e is the internal energy per unit mass, $v_{lk} = g_{li} v^i_{\cdot k}$ the covariant components of the micro-gyration tensor, $v_{l,k} = g_{li} v^i_{,k}$ the covariant components of the velocity gradient, $v_{lm,k} = g_{li} v^i_{\cdot m,k}$ the covariant components of the covariant derivative of the micro-gyration tensor, g_{il} are covariant coefficients of the metric tensor in the current configuration $\mathscr{B}$, q^k is the heat flux vector, r is the heat supply per unit mass, ψ is the Helmholtz free energy per unit mass, η is the entropy per unit mass, and θ is the absolute temperature. Note that the balance of first moment of momentum is more general than the balance of angular momentum (or "moment of momentum" Eringen, 1962), such that its skew-symmetric part is the angular momentum balance of a micropolar continuum. Recall that the Cauchy stress σ'^{ml} over the micro-element is symmetric because the balance of angular momentum is satisfied over the micro-element (Eringen and Suhubi, 1964).

Physically, the micro-stress $\boldsymbol{s}$ defined in (18) as the volume average of the Cauchy stress $\boldsymbol{\sigma}'$ over the micro-element, can be interpreted in the context of its difference with the unsymmetric Cauchy stress as $\boldsymbol{s} - \boldsymbol{\sigma}$ (Mindlin (1964) called this the "relative stress"). This is the energy conjugate driving stress for the micro-deformation $\boldsymbol{\chi}$ through its micro-gyration tensor $\boldsymbol{v} = \dot{\boldsymbol{\chi}}\boldsymbol{\chi}^{-1}$ in (19), and also the reduced dissipation inequality in the intermediate configuration (45) and (48) as $\overline{\boldsymbol{\Sigma}} - \overline{\boldsymbol{S}}$ (the analogous stress difference in $\overline{\mathscr{B}}$). In fact, we do not solve for $\boldsymbol{s}$ or $\overline{\boldsymbol{\Sigma}}$ directly, but constitutively we solve for the difference $\boldsymbol{s} - \boldsymbol{\sigma}$ or $\overline{\boldsymbol{\Sigma}} - \overline{\boldsymbol{S}}$ (see (68)). The higher order stress $\boldsymbol{m}$ is analogous to the double stress $\boldsymbol{\mu}$ in Mindlin (1964) with physical components of micro-stretch, micro-shear, and micro-rotation shown in his Fig. 2. For example, m^{112} is the higher order shear stress in the x_2-direction based on a stretch in the x_1-direction. Using the volume average definition in (24) for m^{klm}, we have $m^{112} \overset{\text{def}}{=} (1/dv) \int_{dv} \sigma'^{11} \xi^2 \, dv'$, where σ'^{11} is the normal micro-element stress in the x_1-direction, and ξ^2 is the shear couple in the x_2-direction.

The remainder of the paper focusses on the Clausius–Duhem inequality mapped to the intermediate configuration to identify evolution equations for various plastic deformation rates that must be defined constitutively, and their appropriate conjugate stress arguments in $\overline{\mathscr{B}}$, and then an example for J_2 plasticity and linear isotropic elasticity, as well as an anti-plane shear form.

4. Clausius–Duhem inequality in $\overline{\boldsymbol{B}}$

From a materials modeling perspective, it is oftentimes preferred to write the Clausius–Duhem inequality in the intermediate configuration $\overline{\mathscr{B}}$, which is considered elastically unloaded, and formulate constitutive equations there. The physical motivation lies with earlier work by Kondo (1952), Bilby et al. (1955), Kröner (1960), and others, who viewed dislocations in crystals as defects with associated local elastic deformation, where macroscopic elastic deformation could be applied and removed without disrupting the dislocation structure of a crystal. More recent models extend this concept, such as papers by Clayton et al. (2005, 2006) and references therein. The intermediate configuration $\overline{\mathscr{B}}$ can be considered a "reference" material configuration in which fabric/texture anisotropy and other inelastic material properties can be defined. Thus, details on the mapping to $\overline{\mathscr{B}}$ are given in this section. Recall that the Clausius–Duhem inequality in (20) was written using localization of an integral over the current configuration $\mathscr{B}$, such as

$$\int_{\mathscr{B}} \left[-\rho(\dot{\psi} + \eta\dot{\theta}) + \sigma^{kl}(v_{l,k} - v_{lk}) + s^{kl} v_{lk} + m^{klm} v_{lm,k} + \frac{1}{\theta} q^k \theta_{,k} \right] dv \geqslant 0 \tag{21}$$

Using the Piola transform $\sigma'^{kl} = F^{e'k}_{\cdot\overline{K}} \overline{S}^{\overline{K}\overline{L}} F^{e'l}_{\cdot\overline{L}} / J^{e'}$, the following mappings of the volume-averaged micro-stress and higher order couple stress terms are obtained as

$$s^{kl} dv \overset{\text{def}}{=} \int_{dv} \sigma'^{kl} \, dv' = \int_{d\overline{V}} \frac{1}{J^{e'}} F^{e'k}_{\cdot\overline{K}} \overline{S}^{\overline{K}\overline{L}} F^{e'l}_{\cdot\overline{L}} J^{e'} d\overline{V}' = F^{ek}_{\cdot\overline{K}} F^{el}_{\cdot\overline{L}} \overline{\Sigma}^{\overline{K}\overline{L}} d\overline{V}$$

$$\overline{\Sigma}^{\overline{K}\overline{L}} d\overline{V} \overset{\text{def}}{=} (F^{e-1})^{\overline{K}}_{\cdot k} (F^{e-1})^{\overline{L}}_{\cdot l} \int_{d\overline{V}} F^{e'k}_{\cdot\overline{i}} F^{e'l}_{\cdot\overline{j}} \overline{S}^{\overline{i}\overline{j}} d\overline{V}' \tag{22}$$

$$\int_{\mathscr{B}} v_{lm,k} m^{klm} dv = \int_{\overline{\mathscr{B}}} v_{lm,k} F^{ek}_{\cdot\overline{K}} F^{el}_{\cdot\overline{L}} \chi^{em}_{\cdot\overline{M}} \overline{M}^{\overline{K}\overline{L}\overline{M}} d\overline{V}$$

$$\overline{M}^{\overline{K}\overline{L}\overline{M}} d\overline{V} \overset{\text{def}}{=} (F^{e-1})^{\overline{K}}_{\cdot i} (F^{e-1})^{\overline{L}}_{\cdot j} \int_{d\overline{V}} F^{e'k}_{\cdot\overline{i}} F^{e'l}_{\cdot\overline{j}} \overline{S}^{\overline{i}\overline{j}} \overline{\Xi}^{\overline{M}} d\overline{V}' \tag{23}$$

where $\overline{S}^{\overline{K}\overline{L}}$ is the symmetric second Piola–Kirchhoff stress in the micro-element intermediate configuration (over $d\overline{V}$), $\overline{\Sigma}^{\overline{K}\overline{L}}$ is the symmetric second Piola–Kirchhoff micro-stress in the intermediate configuration $\overline{\mathscr{B}}$, $\overline{M}^{\overline{K}\overline{L}\overline{M}}$ is the higher order couple stress written in the intermediate configuration, and $\overline{N}_{\overline{K}}$ are the covariant components of the unit normal on $d\overline{A}$. In general, $\boldsymbol{F}^{e'} \neq \boldsymbol{F}^e$, but the constitutive equations in Section 7 do not require that $\boldsymbol{F}^{e'}$ be defined or solved. We have used a volume-average definition for the higher order couple stress (rather than an area-average), such as

$$m^{klm} dv \overset{\text{def}}{=} \int_{dv} \sigma'^{kl} \xi^m \, dv' = \int_{d\overline{V}} F^{e'k}_{\cdot\overline{K}} F^{e'l}_{\cdot\overline{L}} \chi^{em}_{\cdot\overline{M}} \left(\overline{S}^{\overline{K}\overline{L}} \overline{\Xi}^{\overline{M}} \right) d\overline{V}' \tag{24}$$

$$= F^{ek}_{\cdot\overline{K}} F^{el}_{\cdot\overline{L}} \chi^{em}_{\cdot\overline{M}} \overline{M}^{\overline{K}\overline{L}\overline{M}} d\overline{V} \tag{25}$$

The result for expressing the Clausius–Duhem inequality in the intermediate configuration is the same whether we use an area- or volume-average definition for m^{klm}. The volume-average definition becomes useful when homogenizing directly micro-element stress σ'^{kl} and relative position vector ξ^m over a representative volume to calculate m^{klm}, say in a multiscale modeling method. Using the mappings for ρ and dv, and the Piola transform on q^k, the Clausius–Duhem inequality can be rewritten in the intermediate configuration as

$$\int_{\overline{\mathscr{B}}}\Big[-\bar{\rho}\Big(\dot{\bar{\psi}}+\bar{\eta}\dot{\theta}\Big)+J^e\sigma^{kl}(v_{l,k}-v_{lk})+J^e s^{kl}v_{lk} +v_{lm,k}\Big(F^{ek}_{\cdot\overline{K}}F^{el}_{\cdot\overline{L}}\chi^{em}_{\cdot\overline{M}}\overline{M}^{\overline{K}\overline{L}\overline{M}}\Big)+\frac{1}{\theta}\overline{Q}^{\overline{K}}\theta_{,\overline{K}}\Big]d\overline{V}\geqslant 0 \tag{26}$$

Individual stress power terms in (26) can be additively decomposed into elastic and plastic parts based on (7)–(9). Using (9), the higher order couple stress power can be written as

$$\left.\begin{aligned}v_{lm,k}\Big(F^{ek}_{\cdot\overline{K}}F^{el}_{\cdot\overline{L}}\chi^{em}_{\cdot\overline{M}}\overline{M}^{\overline{K}\overline{L}\overline{M}}\Big)&=\overline{M}^{\overline{K}\overline{L}\overline{M}}F^{el}_{\cdot\overline{L}}\Big(g_{la}\dot{\chi}^{ea}_{\cdot\overline{M},\overline{K}}-v^e_{ln}\chi^{en}_{\cdot\overline{M},\overline{K}}\Big)\Big\}\text{elastic}\\ &+M^{\overline{K}\overline{L}\overline{M}}F^{el}_{\cdot\overline{L}}\Big(-v^p_{ln}\chi^{en}_{\cdot\overline{M},\overline{K}}\\ &+g_{la}\Big[\chi^{ea}_{\cdot\overline{C},\overline{K}}\dot{\chi}^{p\overline{C}}_{\cdot A}+\chi^{ea}_{\cdot\overline{D}}\dot{\chi}^{p\overline{D}}_{\cdot A,\overline{K}}-\chi^{ea}_{\cdot\overline{B}}\overline{L}^{\chi,p\overline{B}}_{\cdot\overline{E}}\chi^{p\overline{E}}_{\cdot A,\overline{K}}\Big](\chi^{p-1})^{A}_{\cdot\overline{M}}\Big)\Big\}\text{plastic}\end{aligned}\right. \tag{27}$$

where the covariant derivative with respect to the intermediate configuration $\overline{\mathscr{B}}$ can be defined as $(\bullet)_{,\overline{K}}\overset{\text{def}}{=}(\bullet)_{,k}F^{ek}_{\cdot\overline{K}}$, $v^e_{ln}=g_{la}v^{ea}_{\cdot n}$, and $v^p_{ln}=g_{la}v^{pa}_{\cdot n}$. The other stress power terms using (7) and (8) are written as

$$J^e\sigma^{kl}v_{l,k}=\underbrace{F^{el}_{\cdot\overline{L}}g_{lk}\dot{F}^{ek}_{\cdot\overline{K}}\overline{S}^{\overline{K}\overline{L}}}_{\text{elastic}}+\underbrace{\overline{C}^e_{\overline{L}\overline{B}}\overline{L}^{p\overline{B}}_{\cdot\overline{K}}\overline{S}^{\overline{K}\overline{L}}}_{\text{plastic}} \tag{28}$$

$$J^e\sigma^{kl}v_{lk}=\underbrace{\Big(F^{el}_{\cdot\overline{L}}v^e_{lk}F^{ek}_{\cdot\overline{K}}\Big)\overline{S}^{\overline{K}\overline{L}}}_{\text{elastic}}+\underbrace{\overline{\Psi}^e_{\overline{I}\overline{E}}\overline{L}^{\chi,p\overline{E}}_{\cdot\overline{F}}(\chi^{e-1})^{\overline{F}}_{\cdot k}F^{ek}_{\cdot\overline{K}}\overline{S}^{\overline{K}\overline{L}}}_{\text{plastic}} \tag{29}$$

$$J^e s^{kl}v_{lk}=\underbrace{\Big(F^{el}_{\cdot\overline{L}}v^e_{lk}F^{ek}_{\cdot\overline{K}}\Big)\overline{\Sigma}^{\overline{K}\overline{L}}}_{\text{elastic}}+\underbrace{\overline{\Psi}^e_{\overline{L}\overline{E}}\overline{L}^{\chi,p\overline{E}}_{\cdot\overline{F}}(\chi^{e-1})^{\overline{F}}_{\cdot k}F^{ek}_{\cdot\overline{K}}\overline{\Sigma}^{\overline{K}\overline{L}}}_{\text{plastic}} \tag{30}$$

where $\overline{C}^e_{\overline{L}\overline{B}}=F^{el}_{\cdot\overline{L}}g_{la}F^{ea}_{\cdot\overline{B}}$ are the covariant components of the right elastic Cauchy–Green tensor $\overline{\boldsymbol{C}}^e=\boldsymbol{F}^{eT}\boldsymbol{F}^e$ in $\overline{\mathscr{B}}$, and $\overline{\Psi}^e_{\overline{L}\overline{E}}=F^{el}_{\cdot\overline{L}}g_{la}\chi^{ea}_{\cdot\overline{E}}$ are the covariant components of an elastic deformation measure in $\overline{\mathscr{B}}$ as $\overline{\boldsymbol{\Psi}}^e=\boldsymbol{F}^{eT}\boldsymbol{\chi}^e$ (cf. Appendix A).

5. Constitutive model form and reduced dissipation inequality

Similar to Eringen and Suhubi (1964) for a micromorphic elastic material, the Helmholtz free energy function in $\overline{\mathscr{B}}$ is assumed to take the following functional form for micromorphic elastoplasticity as

$$\begin{aligned}&\bar{\rho}\bar{\psi}(\boldsymbol{F}^e,\boldsymbol{\chi}^e,\bar{\boldsymbol{\nabla}}\boldsymbol{\chi}^e,\overline{\boldsymbol{Z}},\overline{\boldsymbol{Z}}^{\chi},\bar{\boldsymbol{\nabla}}\overline{\boldsymbol{Z}}^{\chi},\theta)\\ &\bar{\rho}\bar{\psi}\Big(F^{ek}_{\cdot\overline{K}},\chi^{ek}_{\cdot\overline{K}},\chi^{ek}_{\cdot\overline{M},\overline{K}},\overline{Z}^{\overline{K}},\overline{Z}^{\chi\overline{K}},\overline{Z}^{\overline{K}}_{\cdot\overline{L}},\theta\Big)\end{aligned} \tag{31}$$

where $\overline{Z}^{\overline{K}}$ is a vector of macro-strain-like ISVs in $\overline{\mathscr{B}}$, $\overline{Z}^{\chi\overline{K}}$ is a vector of micro-strain-like ISVs, and $\overline{Z}^{\overline{K}}_{\cdot\overline{L}}$ is a covariant derivative of a vector of micro-strain-like ISVs. Then, by the chain rule

$$\begin{aligned}\frac{D(\bar{\rho}\bar{\psi})}{Dt}&=\frac{\partial(\bar{\rho}\bar{\psi})}{\partial F^{ek}_{\cdot\overline{K}}}\dot{F}^{ek}_{\cdot\overline{K}}+\frac{\partial(\bar{\rho}\bar{\psi})}{\partial\chi^{ek}_{\cdot\overline{K}}}\dot{\chi}_{\cdot\overline{K}^{ek}}+\frac{\partial(\bar{\rho}\bar{\psi})}{\partial\chi^{ek}_{\cdot\overline{M},\overline{K}}}\frac{D(\chi^{ek}_{\cdot\overline{M},\overline{K}})}{Dt}\\ &+\frac{\partial(\bar{\rho}\bar{\psi})}{\partial\overline{Z}^{\overline{K}}}\dot{\overline{Z}}^{\overline{K}}+\frac{\partial(\bar{\rho}\bar{\psi})}{\partial\overline{Z}^{\chi\overline{K}}}\dot{\overline{Z}}^{\chi\overline{K}}+\frac{\partial(\bar{\rho}\bar{\psi})}{\partial\overline{Z}^{\overline{K}}_{\cdot\overline{L}}}\frac{D\Big(\overline{Z}^{\overline{K}}_{\cdot\overline{L}}\Big)}{Dt}+\frac{\partial(\bar{\rho}\bar{\psi})}{\partial\theta}\dot{\theta}\end{aligned} \tag{32}$$

where an artifact of the "free energy per unit mass" assumption is that

$$\frac{D(\bar{\rho}\bar{\psi})}{Dt}=\dot{\bar{\rho}}\bar{\psi}+\bar{\rho}\dot{\bar{\psi}}=-(\bar{\rho}\bar{\psi})\frac{\dot{J}^p}{J^p}+\bar{\rho}\dot{\bar{\psi}}\Rightarrow\bar{\rho}\dot{\bar{\psi}}=(\bar{\rho}\bar{\psi})\frac{\dot{J}^p}{J^p}+\frac{D(\bar{\rho}\bar{\psi})}{Dt} \tag{33}$$

where we used the result $\dot{\bar{\rho}}=D(\rho_0/J^p)/Dt=-\bar{\rho}\dot{J}^p/J^p$. Substituting (27)–(30) and (32) and (33) into (26), and using the Coleman and Noll (1963) argument for independent rate processes (independent $\dot{F}^{ek}_{\cdot\overline{K}}$, $\dot{\chi}^{ek}_{\cdot\overline{K}}$, $D(\chi^{ek}_{\cdot\overline{M},\overline{K}})/Dt$, and $\dot{\theta}$), the Clausius–Duhem inequality is satisfied if the following constitutive equations hold:

$$\overline{S}^{\overline{K}\overline{L}}=\frac{\partial(\bar{\rho}\bar{\psi})}{\partial F^{ek}_{\cdot\overline{K}}}g^{kl}(F^{e-1})^{\overline{L}}_{\cdot l} \tag{34}$$

$$\begin{aligned}\overline{\Sigma}^{\overline{K}\overline{L}}&=\frac{\partial(\bar{\rho}\bar{\psi})}{\partial F^{ek}_{\cdot\overline{K}}}g^{kl}(F^{e-1})^{\overline{L}}_{\cdot l}+(F^{e-1})^{\overline{K}}_{\cdot c}\chi^{ec}_{\cdot\overline{A}}\frac{\partial(\bar{\rho}\bar{\psi})}{\partial\chi^{ea}_{\cdot\overline{A}}}g^{ab}(F^{e-1})^{\overline{L}}_{\cdot b}\\ &+(F^{e-1})^{\overline{K}}_{\cdot d}\chi^{ed}_{\cdot\overline{M},\overline{E}}\frac{\partial(\bar{\rho}\bar{\psi})}{\partial\chi^{ef}_{\cdot\overline{M},\overline{E}}}g^{fl}(F^{e-1})^{\overline{L}}_{\cdot l}\end{aligned} \tag{35}$$

$$\overline{M}^{\overline{K}\overline{L}\overline{M}}=\frac{\partial(\bar{\rho}\bar{\psi})}{\partial\chi^{ek}_{\cdot\overline{M},\overline{K}}}g^{kl}(F^{e-1})^{\overline{L}}_{\cdot l} \tag{36}$$

$$\bar{\rho}\bar{\eta}=-\frac{\partial(\bar{\rho}\bar{\psi})}{\partial\theta} \tag{37}$$

where g^{kl} are contravariant metric coefficients on $\mathscr{B}$. For comparison to the result reported in Eq. (6.3) of Eringen and Suhubi (1964), we map these stresses to the current configuration, using

$$\sigma^{kl}=\frac{1}{J^e}F^{ek}_{\cdot\overline{K}}\overline{S}^{\overline{K}\overline{L}}F^{el}_{\cdot\overline{L}}=\frac{1}{J^e}F^{ek}_{\cdot\overline{K}}\frac{\partial(\bar{\rho}\bar{\psi})}{\partial F^{ea}_{\cdot\overline{K}}}g^{al} \tag{38}$$

$$s^{kl}=\frac{1}{J^e}F^{ek}_{\cdot\overline{K}}\overline{\Sigma}^{\overline{K}\overline{L}}F^{el}_{\cdot\overline{L}}=\frac{1}{J^e}\left(F^{ek}_{\cdot\overline{K}}\frac{\partial(\bar{\rho}\bar{\psi})}{\partial F^{ea}_{\cdot\overline{K}}}g^{al}+\chi^{ek}_{\cdot\overline{A}}\frac{\partial(\bar{\rho}\bar{\psi})}{\partial\chi^{ea}_{\cdot\overline{A}}}g^{al}+\chi^{ek}_{\cdot\overline{M},\overline{E}}\frac{\partial(\bar{\rho}\bar{\psi})}{\partial\chi^{ef}_{\cdot\overline{M},\overline{E}}}g^{fl}\right)$$

$$m^{klm}=\frac{1}{J^e}F^{ek}_{\cdot\overline{K}}F^{el}_{\cdot\overline{L}}\chi^{em}_{\cdot\overline{M}}\overline{M}^{\overline{K}\overline{L}\overline{M}}=\frac{1}{J^e}\frac{\partial(\bar{\rho}\bar{\psi})}{\partial\chi^{ea}_{\cdot\overline{M},\overline{K}}}g^{al}F^{ek}_{\cdot\overline{K}}\chi^{em}_{\cdot\overline{M}}$$

The equations match those in (6.3) of Eringen and Suhubi (1964) if elastic, i.e. $\boldsymbol{F}^e=\boldsymbol{F}$, $\boldsymbol{\chi}^e=\boldsymbol{\chi}$. We prefer, however, to express the Helmholtz free energy function in terms of invariant—with respect to rigid body motion on the current configuration $\mathscr{B}$—elastic deformation measures, such as the set proposed by Eringen and Suhubi (1964) as

$$\overline{C}^e_{\overline{K}\overline{L}}=F^{ek}_{\cdot\overline{K}}g_{kl}F^{el}_{\cdot\overline{L}},\quad\overline{\Psi}^e_{\overline{K}\overline{L}}=F^{ek}_{\cdot\overline{K}}g_{kl}\chi^{el}_{\cdot\overline{L}},\quad\overline{\Gamma}^e_{\overline{K}\overline{L}\overline{M}}=F^{ek}_{\cdot\overline{K}}g_{kl}\chi_{\cdot\overline{L},\overline{M}} \tag{39}$$

We have good physical interpretation of $\boldsymbol{F}^e$ (and $\boldsymbol{F}^p$) from crystal lattice mechanics (Bilby et al., 1955; Kröner, 1960; Lee and Liu, 1967, 1969), while the elastic micro-deformation $\boldsymbol{\chi}^e$ has its interpretation in Fig. 3 of this paper (elastic deformation of micro-element) and also Fig. 1 of Mindlin (1964) for small strain theory. The covariant derivative (i.e., gradient) of elastic micro-deformation $\bar{\boldsymbol{\nabla}}\boldsymbol{\chi}^e$ has it physical interpretation in Fig. 2 of Mindlin (1964), and was earlier in this paper described, for example, as $(\chi^e)^1_{1,2}$ is the micro-shear gradient in the x_2-direction based on a stretch in the x_1-direction (although directions are not exact here because of the covariant derivative with respect to the intermediate configuration $\overline{\mathscr{B}}$). The Helmholtz free energy function $\bar{\psi}$ per unit mass is then written as

$$\begin{aligned}&\bar{\rho}\bar{\psi}\Big(\overline{\boldsymbol{C}}^e,\overline{\boldsymbol{\Psi}}^e,\overline{\boldsymbol{\Gamma}}^e,\overline{\boldsymbol{Z}},\overline{\boldsymbol{Z}}^{\chi},\bar{\boldsymbol{\nabla}}\overline{\boldsymbol{Z}}^{\chi},\theta\Big)\\ &\bar{\rho}\bar{\psi}\Big(\overline{C}^e_{\overline{K}\overline{L}},\overline{\Psi}^e_{\overline{K}\overline{L}},\overline{\Gamma}^e_{\overline{K}\overline{L}\overline{M}},\overline{Z}^{\overline{K}},\overline{Z}^{\chi\overline{K}},\overline{Z}^{\overline{K}}_{\cdot\overline{L}},\theta\Big)\end{aligned} \tag{40}$$

and the constitutive equations for stress result from (34)–(36) as

$$\overline{S}^{\overline{K}\overline{L}}=2\frac{\partial(\bar{\rho}\bar{\psi})}{\partial\overline{C}^e_{\overline{K}\overline{L}}}+\frac{\partial(\bar{\rho}\bar{\psi})}{\partial\overline{\Psi}^e_{\overline{K}\overline{B}}}\Big(\overline{C}^{e-1}\Big)^{\overline{L}\overline{A}}\overline{\Psi}^e_{\overline{A}\overline{B}}+\frac{\partial(\bar{\rho}\bar{\psi})}{\partial\overline{\Gamma}^e_{\overline{K}\overline{B}\overline{C}}}\Big(\overline{C}^{e-1}\Big)^{\overline{L}\overline{A}}\overline{\Gamma}^e_{\overline{A}\overline{B}\overline{C}} \tag{41}$$

$$\begin{aligned}\overline{\Sigma}^{\overline{K}\overline{L}}&=2\frac{\partial(\bar{\rho}\bar{\psi})}{\partial\overline{C}^e_{\overline{K}\overline{L}}}+2\mathrm{sym}\left[\frac{\partial(\bar{\rho}\bar{\psi})}{\partial\overline{\Psi}^e_{\overline{K}\overline{B}}}\Big(\overline{C}^{e-1}\Big)^{\overline{L}\overline{A}}\overline{\Psi}^e_{\overline{A}\overline{B}}\right]\\ &+2\mathrm{sym}\left[\frac{\partial(\bar{\rho}\bar{\psi})}{\partial\overline{\Gamma}^e_{\overline{K}\overline{B}\overline{C}}}\Big(\overline{C}^{e-1}\Big)^{\overline{L}\overline{A}}\overline{\Gamma}^e_{\overline{A}\overline{B}\overline{C}}\right]\end{aligned} \tag{42}$$

$$\overline{M}^{\overline{K}\overline{L}\overline{M}} = \frac{\partial(\bar{\rho}\bar{\psi})}{\partial \overline{\Gamma}^{e}_{\overline{L}\overline{M}\overline{K}}} \tag{43}$$

where sym[•] denotes the symmetric part, and notice that the metric coefficients cancel, i.e. $g^{al}g_{kl} = \delta^{a}_{k}$. These stress equations (41)–(43) when mapped to the current configuration are the same as Eqs. (6.9)–(11) in Eringen and Suhubi (1964) if there is no plasticity, i.e. $\boldsymbol{F}^{e} = \boldsymbol{F}$ and $\boldsymbol{\chi}^{e} = \boldsymbol{\chi}$. To consider another set of elastic deformation measures and resulting stresses, refer to Appendix B.

The thermodynamically conjugate stress-like ISVs are defined as

$$\overline{Q}_{\overline{K}} \overset{\text{def}}{=} \frac{\partial(\bar{\rho}\bar{\psi})}{\partial \overline{Z}^{\overline{K}}}, \quad \overline{Q}^{\chi}_{\overline{K}} \overset{\text{def}}{=} \frac{\partial(\bar{\rho}\bar{\psi})}{\partial \overline{Z}^{\chi}_{\cdot\overline{K}}}, \quad \left(\overline{Q}^{\nabla\chi}\right)^{\overline{L}}_{\overline{K}} \overset{\text{def}}{=} \frac{\partial(\bar{\rho}\bar{\psi})}{\partial \overline{Z}^{\chi}_{\cdot\overline{L}\overline{K}}} \tag{44}$$

which will be used in the evolution equations for plastic deformation rates, as well as multiple scale yield functions in Section 7.2, where we will assume scalar $\overline{Z}$, $\overline{Z}^{\chi}$, $\overline{\nabla}\overline{Z}^{\chi}$, and $\overline{Q}$, $\overline{Q}^{\chi}$, $\overline{\boldsymbol{Q}}^{\nabla\chi}$. The stress-like ISVs in Section 7 will be physically interpreted as yield stress $\overline{Q}$ and $\overline{Q}^{\chi}$ for macro-plasticity (stress $\overline{\boldsymbol{S}}$ calculated from elastic deformation) and micro-plasticity (stress difference $\overline{\boldsymbol{\Sigma}} - \overline{\boldsymbol{S}}$ calculated from elastic deformation), respectively, while $\overline{\boldsymbol{Q}}^{\nabla\chi}$ is a higher order yield stress for micro-gradient plasticity (higher order stress $\overline{\boldsymbol{M}}$ calculated from gradient elastic deformation).

The remaining terms in the Clausius–Duhem inequality lead to the reduced dissipation inequality expressed in localized form in two ways: (1) Mandel form with Mandel-like stresses (Mandel et al., 1974), and (2) an alternate 'metric' form. Each will lead to different ways of writing the plastic evolution equations, and stresses that are used in these evolution equations. The reduced dissipation inequality in Mandel form is written as

$$\begin{aligned}
&(\bar{\rho}\bar{\psi})\frac{\dot{J}^{p}}{J^{p}} + \frac{1}{\theta}\overline{Q}^{\overline{K}}\theta_{,\overline{K}} - \overline{Q}_{\overline{K}}\dot{\overline{Z}}^{\overline{K}} - \overline{Q}^{\chi}_{\overline{K}}\dot{\overline{Z}}^{\chi\overline{K}} - \left(\overline{Q}^{\nabla\chi}\right)^{\overline{L}}_{\overline{K}}\frac{D\left(\overline{Z}^{\chi\overline{K}}_{\cdot\overline{L}}\right)}{Dt} \\
&\quad + \left(\overline{S}^{\overline{K}\overline{B}}\overline{C}^{e}_{\overline{B}\overline{L}}\right)\overline{L}^{p\overline{L}}_{\cdot\overline{K}} + \left[\left(\overline{C}^{\chi,e-1}\right)^{\overline{K}\overline{N}}\overline{\Psi}^{e}_{\overline{A}\overline{N}}\left(\overline{\Sigma}^{\overline{A}\overline{B}} - \overline{S}^{\overline{A}\overline{B}}\right)\overline{\Psi}^{e}_{\overline{B}\overline{L}}\right]\overline{L}^{\chi,p\overline{L}}_{\cdot\overline{K}} \\
&\quad + \left(\overline{M}^{\overline{K}\overline{L}\overline{M}}\overline{\Psi}^{e}_{\overline{L}\overline{D}}\right)\left\{\overline{L}^{\chi,p\overline{D}}_{\cdot\overline{M},\overline{K}} - 2\text{skw}\left[\overline{L}^{\chi,p\overline{D}}_{\cdot\overline{C}}\left(\overline{\Psi}\right)^{e-1\overline{C}\overline{F}}\overline{\Gamma}^{e}_{\overline{F}\overline{M}\overline{K}}\right]\right\} \geqslant 0
\end{aligned} \tag{45}$$

where $\left(\overline{C}^{\chi,e-1}\right)^{\overline{K}\overline{N}} = (\chi^{e-1})^{\overline{K}}_{\cdot k}g^{kn}(\chi^{e-1})^{\overline{N}}_{\cdot n}$, $\left(\overline{\Psi}^{e-1}\right)^{\overline{C}\overline{F}} = (\chi^{e-1})^{\overline{C}}_{\cdot i}g^{ia}(F^{e-1})^{\overline{F}}_{\cdot a}$, skw[•] denotes the skew-symmetric part defined as

$$2\text{skw}[\bullet] \overset{\text{def}}{=} \left[\overline{L}^{\chi,p\overline{D}}_{\cdot\overline{C}}\left(\overline{\Psi}^{e-1}\right)^{\overline{C}\overline{F}}\overline{\Gamma}^{e}_{\overline{F}\overline{M}\overline{K}}\right] - \left[\overline{L}^{\chi,p\overline{B}}_{\cdot\overline{M}}\left(\overline{\Psi}^{e-1}\right)^{\overline{D}\overline{G}}\overline{\Gamma}^{e}_{\overline{G}\overline{B}\overline{K}}\right] \tag{46}$$

and the covariant derivative of the micro-scale plastic velocity gradient is

$$\overline{L}^{\chi,p\overline{D}}_{\cdot\overline{M},\overline{K}} = \left[\dot{\chi}^{p\overline{D}}_{\cdot B}(\chi^{p-1})^{B}_{\cdot\overline{M}}\right]_{,\overline{K}} = \left(\dot{\chi}^{p\overline{D}}_{\cdot B,\overline{K}} - \overline{L}^{\chi,p\overline{D}}_{\cdot\overline{B}}\chi^{p\overline{B}}_{\cdot B,\overline{K}}\right)(\chi^{p-1})^{B}_{\cdot\overline{M}} \tag{47}$$

The Mandel stresses are $\overline{S}^{\overline{K}\overline{B}}\overline{C}^{e}_{\overline{B}\overline{L}}$, $\left(\overline{C}^{\chi,e-1}\right)^{\overline{K}\overline{N}}\overline{\Psi}^{e}_{\overline{A}\overline{N}}\left(\overline{\Sigma}^{\overline{A}\overline{B}} - \overline{S}^{\overline{A}\overline{B}}\right)\overline{\Psi}^{e}_{\overline{B}\overline{L}}$, and $\overline{M}^{\overline{K}\overline{L}\overline{M}}\overline{\Psi}^{e}_{\overline{L}\overline{D}}$, where the first one is well-known as the "Mandel stress", whereas the second and third are the relative micro-Mandel stress and the higher order Mandel couple stress, respectively. We rewrite the reduced dissipation inequality (45) in an alternate 'metric' form as

$$\begin{aligned}
&(\bar{\rho}\bar{\psi})\frac{\dot{J}^{p}}{J^{p}} + \frac{1}{\theta}\overline{Q}^{\overline{K}}\theta_{,\overline{K}} - \overline{Q}_{\overline{K}}\dot{\overline{Z}}^{\overline{K}} - \overline{Q}^{\chi}_{\overline{K}}\dot{\overline{Z}}^{\chi\overline{K}} - \left(\overline{Q}^{\nabla\chi}\right)^{\overline{L}}_{\overline{K}}\frac{D\left(\overline{Z}^{\chi\overline{K}}_{\cdot\overline{L}}\right)}{Dt} \\
&\quad + \overline{S}^{\overline{K}\overline{L}}\left(\overline{C}^{e}_{\overline{L}\overline{B}}\overline{L}^{p\overline{B}}_{\cdot\overline{K}}\right) + \left(\overline{\Sigma}^{\overline{K}\overline{L}} - \overline{S}^{\overline{K}\overline{L}}\right)\left[\overline{\Psi}^{e}_{\overline{L}\overline{E}}\overline{L}^{\chi,p\overline{E}}_{\cdot\overline{F}}\left(\overline{C}^{\chi,e-1}\right)^{\overline{F}\overline{N}}\overline{\Psi}^{e}_{\overline{K}\overline{N}}\right] \\
&\quad + \overline{M}^{\overline{K}\overline{L}\overline{M}}\left\{\overline{\Psi}^{e}_{\overline{L}\overline{D}}\overline{L}^{\chi,p\overline{D}}_{\cdot\overline{M},\overline{K}} - 2\overline{\Psi}^{e}_{\overline{L}\overline{D}}\text{skw}\left[\overline{L}^{\chi,p\overline{D}}_{\cdot\overline{C}}\left(\overline{\Psi}^{e-1}\right)^{\overline{C}\overline{F}}\overline{\Gamma}^{e}_{\overline{F}\overline{M}\overline{K}}\right]\right\} \geqslant 0
\end{aligned} \tag{48}$$

Appendix A considers various choices for covariant metric coefficients $\overline{G}_{\overline{K}\overline{L}}$, (and contravariant metric $\overline{G}^{\overline{K}\overline{L}}$), that have appeared thus far in the constitutive equations. For example, if $\overline{G}_{\overline{K}\overline{L}} \overset{\text{def}}{=} \overline{C}_{\overline{K}\overline{L}}$ (Clayton et al., 2004) (Appendix A), then the covariant components of $\overline{\boldsymbol{L}}^{p}$ are $\overline{L}^{p}_{\overline{L}\overline{K}} = \overline{G}_{\overline{L}\overline{B}}\overline{L}^{p\overline{B}}_{\cdot\overline{K}} = \overline{C}^{e}_{\overline{L}\overline{B}}\overline{L}^{p\overline{B}}_{\cdot\overline{K}}$ in (48). However, this choice also leads to zero elastic strain $\overline{E}^{e}_{\overline{K}\overline{L}} = 0$, and thus we will assume the intermediate configuration $\overline{\mathscr{B}}$ is Cartesian in the future. If the intermediate configuration is assumed Cartesian, $\overline{L}^{p}_{\overline{L}\overline{K}} = \overline{G}_{\overline{L}\overline{B}}\overline{L}^{p\overline{B}}_{\cdot\overline{K}} = \delta_{\overline{L}\overline{B}}\overline{L}^{p\overline{B}}_{\cdot\overline{K}}$, and there is no difference between superscripts and subscripts.

6. Form of plastic evolution equations

Based on (45), in order to satisfy the reduced dissipation inequality, we can write plastic evolution equations to solve for $F^{p\overline{K}}_{\cdot\overline{K}}$, $\chi^{p\overline{K}}_{\cdot\overline{K}}$, and $\chi^{p\overline{K}}_{\cdot\overline{K},\overline{L}}$ in Mandel stress form as

$$\overline{L}^{p\overline{L}}_{\cdot\overline{K}} = \overline{H}^{\overline{L}}_{\cdot\overline{K}}\left(\overline{\boldsymbol{S}}\overline{\boldsymbol{C}}^{e}, \overline{\boldsymbol{Q}}\right) \qquad \text{solve for } F^{p\overline{K}}_{\cdot\overline{K}} \text{ and } F^{ek}_{\cdot\overline{K}} = F^{k}_{\cdot K}(F^{p-1})^{K}_{\cdot\overline{K}} \tag{49}$$

$$\begin{aligned}
&\overline{L}^{\chi,p\overline{L}}_{\cdot\overline{K}} = \overline{H}^{\chi\overline{L}}_{\cdot\overline{K}}\left(\left(\overline{\boldsymbol{C}}^{\chi,e}\right)^{-1}\overline{\boldsymbol{\Psi}}^{eT}\left(\overline{\boldsymbol{\Sigma}} - \overline{\boldsymbol{S}}\right)\overline{\boldsymbol{\Psi}}^{e}, \overline{\boldsymbol{Q}}^{\chi}\right) \\
&\qquad \text{solve for } \chi^{p\overline{K}}_{\cdot K} \text{ and } \chi^{ek}_{\cdot\overline{K}} = \chi^{k}_{\cdot K}(\chi^{p-1})^{K}_{\cdot\overline{K}}
\end{aligned} \tag{50}$$

$$\begin{aligned}
&\overline{L}^{\chi,p\overline{D}}_{\cdot\overline{M},\overline{K}} - 2\text{skw}\left[\overline{L}^{\chi,p\overline{D}}_{\cdot\overline{C}}\left(\overline{\Psi}^{e-1}\right)^{\overline{C}\overline{F}}\overline{\Gamma}^{e}_{\overline{F}\overline{M}\overline{K}}\right] = \left(\overline{H}^{\nabla\chi}\right)^{\overline{D}}_{\cdot\overline{M}\overline{K}}\left(\overline{\boldsymbol{M}}\overline{\boldsymbol{\Psi}}^{e}, \overline{\boldsymbol{Q}}^{\nabla\chi}\right) \\
&\qquad \text{solve for } \chi^{p\overline{K}}_{\cdot K,\overline{L}} \text{ and } \chi^{ek}_{\cdot\overline{K},\overline{L}} = \left(\chi^{k}_{\cdot K,\overline{L}} - \chi^{ek}_{\cdot\overline{A}}\chi^{p\overline{A}}_{\cdot K,\overline{L}}\right)(\chi^{p-1})^{K}_{\cdot\overline{K}}
\end{aligned} \tag{51}$$

where the arguments in parentheses (•) denote the Mandel stress and stress-like ISV to use in the respective plastic evolution equation, where $\overline{\boldsymbol{H}}, \overline{\boldsymbol{H}}^{\chi}$, and $\overline{\boldsymbol{H}}^{\nabla\chi}$ denote tensor functions for the evolution equations, chosen to ensure that convexity is satisfied, and the dissipation is positive. This can be seen for the evolution equations in (52)–(54) by the constitutive definitions in (70) and (74) and (78) in terms of stress gradients of potential functions (i.e., the yield functions for associative plasticity). In an alternate 'metric' form, from (48), we can solve for the plastic deformation variables as

$$\overline{C}^{e}_{\overline{L}\overline{B}}\overline{L}^{p\overline{B}}_{\cdot\overline{K}} = \overline{H}_{\overline{L}\overline{K}}\left(\overline{\boldsymbol{S}}, \overline{\boldsymbol{Q}}\right) \qquad \text{solve for } F^{p\overline{K}}_{\cdot\overline{K}} \text{ and } F^{ek}_{\cdot\overline{K}} = F^{k}_{\cdot K}(F^{p-1})^{K}_{\cdot\overline{K}} \tag{52}$$

$$\begin{aligned}
&\overline{\Psi}^{e}_{\overline{L}\overline{E}}\overline{L}^{\chi,p\overline{E}}_{\cdot\overline{F}}\left(\overline{C}^{\chi,e-1}\right)^{\overline{F}\overline{N}}\overline{\Psi}^{e}_{\overline{K}\overline{N}} = \overline{H}^{\chi}_{\overline{L}\overline{K}}\left(\overline{\boldsymbol{\Sigma}} - \overline{\boldsymbol{S}}, \overline{\boldsymbol{Q}}^{\chi}\right) \\
&\qquad \text{solve for } \chi^{p\overline{K}}_{\cdot K} \text{ and } \chi^{ek}_{\cdot\overline{K}} = \chi^{k}_{\cdot K}(\chi^{p-1})^{K}_{\cdot\overline{K}}
\end{aligned} \tag{53}$$

$$\begin{aligned}
&\overline{\Psi}^{e}_{\overline{L}\overline{D}}\overline{L}^{\chi,p\overline{D}}_{\cdot\overline{M},\overline{K}} - 2\overline{\Psi}^{e}_{\overline{L}\overline{D}}\text{skw}\left[\overline{L}^{\chi,p\overline{D}}_{\cdot\overline{C}}\left(\overline{\Psi}^{e-1}\right)^{\overline{C}\overline{F}}\overline{\Gamma}^{e}_{\overline{F}\overline{M}\overline{K}}\right] = \overline{H}^{\nabla\chi}_{\overline{L}\overline{M}\overline{K}}\left(\overline{\boldsymbol{M}}, \overline{\boldsymbol{Q}}^{\nabla\chi}\right) \\
&\qquad \text{solve for } \chi^{p\overline{K}}_{\cdot K,\overline{L}} \text{ and } \chi^{ek}_{\cdot\overline{K},\overline{L}} = \left(\chi^{k}_{\cdot K,\overline{L}} - \chi^{ek}_{\cdot\overline{A}}\chi^{p\overline{A}}_{\cdot K,\overline{L}}\right)(\chi^{p-1})^{K}_{\cdot\overline{K}}
\end{aligned} \tag{54}$$

We use this 'metric' form in defining evolution equations in Section 7.2.

Remark 1. The reason that we propose the third plastic evolution equation (51) or (54) to solve for $\chi^{p\overline{K}}_{\cdot K,\overline{L}}$ directly (not calculating a covariant derivative of the tensor $\chi^{p\overline{K}}_{\cdot K}$ from a finite element interpolation of $\boldsymbol{\chi}^{p}$) is to potentially avoid requiring an additional balance equation to solve in weak form by a nonlinear finite element method (refer to Regueiro et al. (2007) and references cited therein). With future finite element implementation and numerical examples, we will attempt to determine whether (51) or (54) leads to an accurate calculation of $\chi^{p\overline{K}}_{\cdot K,\overline{L}}$. In Section 9, a simpler anti-plane shear version of the model demonstrates the two ways for calculating $\overline{\nabla}\boldsymbol{\chi}^{p}$, either by an evolution equation like in (51) or (54), or a finite element interpolation for $\boldsymbol{\chi}^{p}$ and corresponding gradient calculation $\overline{\nabla}\boldsymbol{\chi}^{p}$. Note that in Forest and Sievert (2003), for

their equation (155_3), they also propose a direct evolution of a gradient of plastic microdeformation.

7. Constitutive equations

The constitutive equations for linear isotropic elasticity and J_2 plasticity with scalar ISV hardening/softening are formulated. We define a specific form of the Helmholtz free energy function, yield functions, and evolution equations for ISVs, and then conduct a numerical time integration presented in Section 8. Future work entails implementing the model in a coupled Lagrangian finite element method.

7.1. Helmholtz free energy and stresses

Assuming linear isotropic elasticity and linear relation between stress-like and strain-like ISVs, a quadratic form for the Helmholtz free energy function results as

$$\begin{aligned}\bar{\rho}\bar{\psi} \overset{\text{def}}{=} &\frac{1}{2}\overline{E}^e_{\overline{K}\overline{L}}\overline{A}^{\overline{K}\overline{L}\overline{M}\overline{N}}\overline{E}^e_{\overline{M}\overline{N}} + \frac{1}{2}\overline{\mathscr{E}}^e_{\overline{K}\overline{L}}\overline{B}^{\overline{K}\overline{L}\overline{M}\overline{N}}\overline{\mathscr{E}}^e_{\overline{M}\overline{N}}\\ &+\frac{1}{2}\overline{\Gamma}^e_{\overline{K}\overline{L}\overline{M}}\overline{C}^{\overline{K}\overline{L}\overline{M}\overline{N}\overline{P}\overline{Q}}\overline{\Gamma}^e_{\overline{N}\overline{P}\overline{Q}} + \frac{1}{2}\overline{E}^e_{\overline{K}\overline{L}}\overline{D}^{\overline{K}\overline{L}\overline{M}\overline{N}}\overline{\mathscr{E}}^e_{\overline{M}\overline{N}} + \frac{1}{2}\overline{H}\overline{Z}^2\\ &+\frac{1}{2}\overline{H}^\chi\left(\overline{Z}^\chi\right)^2 + \frac{1}{2}\overline{Z}^\chi_{,\overline{K}}\left(\overline{H}^{\nabla\chi}\right)^{\overline{K}\overline{L}}\overline{Z}^\chi_{,\overline{L}}\end{aligned} \tag{55}$$

Note that the ISVs are scalar variables in this model, which will be related to scalar yield strength of the material at two scales, macro and micro, and $\overline{H}$ and $\overline{H}^\chi$ are scalar hardening/softening parameters, and $\left(\overline{H}^{\nabla\chi}\right)^{\overline{K}\overline{L}}$ is a symmetric second order hardening/softening modulus tensor, which we will assume is isotropic as $\left(\overline{H}^{\nabla\chi}\right)^{\overline{K}\overline{L}} = \overline{H}^{\nabla\chi}\overline{G}^{\overline{K}\overline{L}}$. Elastic strains are defined as (Suhubi and Eringen, 1964) $2\overline{E}^e_{\overline{K}\overline{L}} = \overline{C}^e_{\overline{K}\overline{L}} - \overline{G}_{\overline{K}\overline{L}}$ and $\overline{\mathscr{E}}^e_{\overline{K}\overline{L}} = \overline{\Psi}^e_{\overline{K}\overline{L}} - \overline{G}_{\overline{K}\overline{L}}$. The elastic moduli are defined for isotropic linear elasticity, after manipulation of equations in Suhubi and Eringen (1964) as

$$\overline{A}^{\overline{K}\overline{L}\overline{M}\overline{N}} = \lambda\overline{G}^{\overline{K}\overline{L}}\overline{G}^{\overline{M}\overline{N}} + \mu\left(\overline{G}^{\overline{K}\overline{M}}\overline{G}^{\overline{L}\overline{N}} + \overline{G}^{\overline{K}\overline{N}}\overline{G}^{\overline{L}\overline{M}}\right) \tag{56}$$

$$\begin{aligned}\overline{B}^{\overline{K}\overline{L}\overline{M}\overline{N}} = &(\eta-\tau)\overline{G}^{\overline{K}\overline{L}}\overline{G}^{\overline{M}\overline{N}} + \kappa\overline{G}^{\overline{K}\overline{M}}\overline{G}^{\overline{L}\overline{N}} + \nu\overline{G}^{\overline{K}\overline{N}}\overline{G}^{\overline{L}\overline{M}}\\ &-\sigma\left(\overline{G}^{\overline{K}\overline{M}}\overline{G}^{\overline{L}\overline{N}} + \overline{G}^{\overline{K}\overline{N}}\overline{G}^{\overline{L}\overline{M}}\right)\end{aligned} \tag{57}$$

$$\begin{aligned}\overline{C}^{\overline{K}\overline{L}\overline{M}\overline{N}\overline{P}\overline{Q}} = &\tau_1\left(\overline{G}^{\overline{K}\overline{L}}\overline{G}^{\overline{M}\overline{N}}\overline{G}^{\overline{P}\overline{Q}} + \overline{G}^{\overline{K}\overline{Q}}\overline{G}^{\overline{L}\overline{M}}\overline{G}^{\overline{N}\overline{P}}\right)\\ &+\tau_2\left(\overline{G}^{\overline{K}\overline{L}}\overline{G}^{\overline{M}\overline{P}}\overline{G}^{\overline{N}\overline{Q}} + \overline{G}^{\overline{K}\overline{M}}\overline{G}^{\overline{L}\overline{Q}}\overline{G}^{\overline{N}\overline{P}}\right)\\ &+\tau_3\overline{G}^{\overline{K}\overline{L}}\overline{G}^{\overline{M}\overline{Q}}\overline{G}^{\overline{N}\overline{P}} + \tau_4\overline{G}^{\overline{K}\overline{N}}\overline{G}^{\overline{L}\overline{M}}\overline{G}^{\overline{P}\overline{Q}}\\ &+\tau_5\left(\overline{G}^{\overline{K}\overline{M}}\overline{G}^{\overline{L}\overline{N}}\overline{G}^{\overline{P}\overline{Q}} + \overline{G}^{\overline{K}\overline{P}}\overline{G}^{\overline{L}\overline{M}}\overline{G}^{\overline{N}\overline{Q}}\right)\\ &+\tau_6\overline{G}^{\overline{K}\overline{M}}\overline{G}^{\overline{L}\overline{P}}\overline{G}^{\overline{N}\overline{Q}} + \tau_7\overline{G}^{\overline{K}\overline{N}}\overline{G}^{\overline{L}\overline{P}}\overline{G}^{\overline{M}\overline{Q}}\\ &+\tau_8\left(\overline{G}^{\overline{K}\overline{P}}\overline{G}^{\overline{L}\overline{Q}}\overline{G}^{\overline{M}\overline{N}} + \overline{G}^{\overline{K}\overline{Q}}\overline{G}^{\overline{L}\overline{N}}\overline{G}^{\overline{M}\overline{P}}\right)\\ &+\tau_9\overline{G}^{\overline{K}\overline{N}}\overline{G}^{\overline{L}\overline{Q}}\overline{G}^{\overline{M}\overline{P}} + \tau_{10}\overline{G}^{\overline{K}\overline{P}}\overline{G}^{\overline{L}\overline{N}}\overline{G}^{\overline{M}\overline{Q}}\\ &+\tau_{11}\overline{G}^{\overline{K}\overline{Q}}\overline{G}^{\overline{L}\overline{P}}\overline{G}^{\overline{M}\overline{N}}\end{aligned} \tag{58}$$

$$\overline{D}^{\overline{K}\overline{L}\overline{M}\overline{N}} = \tau\overline{G}^{\overline{K}\overline{L}}\overline{G}^{\overline{M}\overline{N}} + \sigma\left(\overline{G}^{\overline{K}\overline{M}}\overline{G}^{\overline{L}\overline{N}} + \overline{G}^{\overline{K}\overline{N}}\overline{G}^{\overline{L}\overline{M}}\right) \tag{59}$$

where $\overline{A}^{\overline{K}\overline{L}\overline{M}\overline{N}}$ and $\overline{D}^{\overline{K}\overline{L}\overline{M}\overline{N}}$ have major and minor symmetry, while $\overline{B}^{\overline{K}\overline{L}\overline{M}\overline{N}}$ and $\overline{C}^{\overline{K}\overline{L}\overline{M}\overline{N}\overline{P}\overline{Q}}$ have only major symmetry, and the elastic parameters are λ, μ, η, τ, κ, ν, σ, $\tau_1,\ldots,\tau_{11}$. Note that the units for $\tau_1,\ldots,\tau_{11}$ are stress $*$ length^2 (Pa m^2), thus there is a built in length scale to these elastic parameters for the higher order stress. The elastic modulus tensors $\overline{A}^{\overline{K}\overline{L}\overline{M}\overline{N}}$, $\overline{B}^{\overline{K}\overline{L}\overline{M}\overline{N}}$, and $\overline{D}^{\overline{K}\overline{L}\overline{M}\overline{N}}$ are not the same as in Eringen (1999) because different elastic strain measures were used, but the higher order elastic modulus tensor $\overline{C}^{\overline{K}\overline{L}\overline{M}\overline{N}\overline{P}\overline{Q}}$ is the same. Note that $\overline{\boldsymbol{A}}$ is the typical linear isotropic elastic tangent modulus tensor, and λ and μ are the Lamé parameters. After some algebra using (41)–(44) and (55), it can be shown that the stress constitutive relations are

$$\begin{aligned}\overline{S}^{\overline{K}\overline{L}} = &\overline{A}^{\overline{K}\overline{L}\overline{M}\overline{N}}\overline{E}^e_{\overline{M}\overline{N}} + \overline{D}^{\overline{K}\overline{B}\overline{M}\overline{N}}\overline{\mathscr{E}}^e_{\overline{M}\overline{N}}\\ &+\left(\overline{D}^{\overline{K}\overline{B}\overline{M}\overline{N}}\overline{E}^e_{\overline{M}\overline{N}} + \overline{B}^{\overline{K}\overline{B}\overline{M}\overline{N}}\overline{\mathscr{E}}^e_{\overline{M}\overline{N}}\right)\left[\left(\overline{C}^{e-1}\right)^{\overline{L}\overline{A}}\left(\overline{\mathscr{E}}^e_{\overline{A}\overline{B}} + \overline{G}_{\overline{A}\overline{B}}\right)\right]\\ &+\overline{C}^{\overline{K}\overline{B}\overline{C}\overline{N}\overline{P}\overline{Q}}\overline{\Gamma}^e_{\overline{N}\overline{P}\overline{Q}}\left(\overline{C}^{e-1}\right)^{\overline{L}\overline{Q}}\overline{\Gamma}^e_{\overline{Q}\overline{B}\overline{C}}\end{aligned} \tag{60}$$

$$\begin{aligned}\overline{\Sigma}^{\overline{K}\overline{L}} = &\overline{A}^{\overline{K}\overline{L}\overline{M}\overline{N}}\overline{E}^e_{\overline{M}\overline{N}} + \overline{D}^{\overline{K}\overline{B}\overline{M}\overline{N}}\overline{\mathscr{E}}^e_{\overline{M}\overline{N}}\\ &+2\mathrm{sym}\left\{\left(\overline{D}^{\overline{K}\overline{L}\overline{M}\overline{N}}\overline{E}^e_{\overline{M}\overline{N}} + \overline{B}^{\overline{K}\overline{B}\overline{M}\overline{N}}\overline{\mathscr{E}}^e_{\overline{M}\overline{N}}\right)\left[\left(\overline{C}^{e-1}\right)^{\overline{L}\overline{A}}\left(\overline{\mathscr{E}}^e_{\overline{A}\overline{B}} + \overline{G}_{\overline{A}\overline{B}}\right)\right]\right.\\ &\left.+\overline{C}^{\overline{K}\overline{B}\overline{C}\overline{N}\overline{P}\overline{Q}}\overline{\Gamma}^e_{\overline{N}\overline{P}\overline{Q}}\left(\overline{C}^{e-1}\right)^{\overline{L}\overline{Q}}\overline{\Gamma}^e_{\overline{Q}\overline{B}\overline{C}}\right\}\end{aligned} \tag{61}$$

$$\overline{M}^{\overline{K}\overline{L}\overline{M}} = \overline{C}^{\overline{K}\overline{L}\overline{M}\overline{N}\overline{P}\overline{Q}}\overline{\Gamma}^e_{\overline{N}\overline{P}\overline{Q}} \tag{62}$$

$$\overline{Q} = \overline{H}\overline{Z} \tag{63}$$

$$\overline{Q}^\chi = \overline{H}^\chi\overline{Z}^\chi \tag{64}$$

$$\left(\overline{Q}^\chi\right)^{\overline{L}} = \overline{H}^{\nabla\chi}\overline{Z}^\chi_{,\overline{A}}\overline{G}^{\overline{A}\overline{L}} \tag{65}$$

Note that the units for $\overline{H}^{\nabla\chi}$ are stress $*$ length^2 (Pa m^2), thus there is a built in length scale to this hardening/softening parameter for the higher order stress-like ISV. Assuming elastic deformations are small, we ignore quadratic terms in (60) and (61), leading to the simplified stress constitutive equations for $\overline{S}^{\overline{K}\overline{L}}$ and $\overline{\Sigma}^{\overline{K}\overline{L}}$ as

$$\begin{aligned}\overline{S}^{\overline{K}\overline{L}} &= \left(\overline{A}^{\overline{K}\overline{L}\overline{M}\overline{N}} + \overline{D}^{\overline{K}\overline{L}\overline{M}\overline{N}}\right)\overline{E}^e_{\overline{M}\overline{N}} + \left(\overline{B}^{\overline{K}\overline{L}\overline{M}\overline{N}} + \overline{D}^{\overline{K}\overline{L}\overline{M}\overline{N}}\right)\overline{\mathscr{E}}^e_{\overline{M}\overline{N}}\\ &= (\lambda+\tau)\left(\overline{G}^{\overline{M}\overline{N}}\overline{E}^e_{\overline{M}\overline{N}}\right)\overline{G}^{\overline{K}\overline{L}} + 2(\mu+\sigma)\overline{G}^{\overline{K}\overline{N}}\overline{G}^{\overline{L}\overline{M}}\overline{E}^e_{\overline{M}\overline{N}}\\ &\quad+\eta\left(\overline{G}^{\overline{M}\overline{N}}\overline{\mathscr{E}}^e_{\overline{M}\overline{N}}\right)\overline{G}^{\overline{K}\overline{L}} + \kappa\overline{G}^{\overline{K}\overline{M}}\overline{G}^{\overline{L}\overline{N}}\overline{\mathscr{E}}^e_{\overline{M}\overline{N}} + \nu\overline{G}^{\overline{K}\overline{N}}\overline{G}^{\overline{L}\overline{M}}\overline{\mathscr{E}}^e_{\overline{M}\overline{N}}\end{aligned} \tag{66}$$

$$\begin{aligned}\overline{\Sigma}^{\overline{K}\overline{L}} = &(\lambda+2\tau)\left(\overline{G}^{\overline{M}\overline{N}}\overline{E}^e_{\overline{M}\overline{N}}\right)\overline{G}^{\overline{K}\overline{L}} + 2(\mu+2\sigma)\overline{G}^{\overline{K}\overline{N}}\overline{G}^{\overline{L}\overline{M}}\overline{E}^e_{\overline{M}\overline{N}}\\ &+(2\eta-\tau)\left(\overline{G}^{\overline{M}\overline{N}}\overline{\mathscr{E}}^e_{\overline{M}\overline{N}}\right)\overline{G}^{\overline{K}\overline{L}} + 2(k+\nu-\sigma)\mathrm{sym}\left(\overline{G}^{\overline{K}\overline{M}}\overline{G}^{\overline{L}\overline{N}}\overline{\mathscr{E}}^e_{\overline{M}\overline{N}}\right)\end{aligned} \tag{67}$$

Note that the stress difference used in (53) then becomes

$$\begin{aligned}\overline{\Sigma}^{\overline{K}\overline{L}} - \overline{S}^{\overline{K}\overline{L}} = &\tau\left(\overline{G}^{\overline{M}\overline{N}}\overline{E}^e_{\overline{M}\overline{N}}\right)\overline{G}^{\overline{K}\overline{L}} + 2\sigma\overline{G}^{\overline{K}\overline{N}}\overline{G}^{\overline{L}\overline{M}}\overline{E}^e_{\overline{M}\overline{N}}\\ &+(\eta-\tau)\left(\overline{G}^{\overline{M}\overline{N}}\overline{\mathscr{E}}^e_{\overline{M}\overline{N}}\right)\overline{G}^{\overline{K}\overline{L}} + (\nu-\sigma)\overline{G}^{\overline{K}\overline{M}}\overline{G}^{\overline{L}\overline{N}}\overline{\mathscr{E}}^e_{\overline{M}\overline{N}}\\ &+(\kappa-\sigma)\overline{G}^{\overline{L}\overline{M}}\overline{G}^{\overline{K}\overline{N}}\overline{\mathscr{E}}^e_{\overline{M}\overline{N}}\end{aligned} \tag{68}$$

7.2. Yield functions and evolution equations

In this section, three levels of plastic yield functions are defined based on the three conjugate stress-plastic-power terms appearing in the reduced dissipation inequality (48), with the intent to define the plastic deformation evolution equations such that (48) is satisfied. Recall the plastic power terms in (48) come naturally from the kinematic assumptions $\boldsymbol{F} = \boldsymbol{F}^e\boldsymbol{F}^p$ and $\boldsymbol{\chi} = \boldsymbol{\chi}^e\boldsymbol{\chi}^p$, and from the Helmholtz free energy function dependence on the invariant elastic deformation measures $\overline{\boldsymbol{C}}^e$, $\overline{\boldsymbol{\Psi}}^e$, $\overline{\boldsymbol{\Gamma}}^e$, and the plastic strain-like ISVs $\overline{Z}$, $\overline{Z}^\chi$, and $\bar{\nabla}\overline{Z}^\chi$.

7.2.1. Macro-scale plasticity

For macro-scale plasticity, we write the yield function $\overline{F}$ as

$$\overline{F}\left(\overline{\boldsymbol{S}},\bar{\alpha}\right)\overset{\text{def}}{=}\left\|\text{dev}\overline{\boldsymbol{S}}\right\|-\bar{\alpha}\leqslant 0 \tag{69}$$

$$\left\|\text{dev}\overline{\boldsymbol{S}}\right\|=\sqrt{\left(\text{dev}\overline{\boldsymbol{S}}\right):\left(\text{dev}\overline{\boldsymbol{S}}\right)}$$

$$\left(\text{dev}\overline{\boldsymbol{S}}\right):\left(\text{dev}\overline{\boldsymbol{S}}\right)=\left(\text{dev}\overline{S}^{\bar{I}\bar{J}}\right)\left(\text{dev}\overline{S}_{\bar{I}\bar{J}}\right)=\left(\text{dev}\overline{S}^{\bar{I}\bar{J}}\right)\overline{G}_{\bar{M}\bar{I}}\overline{G}_{\bar{N}\bar{J}}\left(\text{dev}\overline{S}^{\bar{M}\bar{N}}\right)$$

$$\text{dev}\overline{S}^{\bar{I}\bar{J}}=\overline{S}^{\bar{I}\bar{J}}-\left(\frac{1}{3}\overline{C}^{e}_{\bar{A}\bar{B}}\overline{S}^{\bar{A}\bar{B}}\right)\left(\overline{C}^{e-1}\right)^{\bar{I}\bar{J}}$$

where $\bar{\alpha}$ is the macro-yield strength (i.e., stress-like ISV $\overline{Q}\overset{\text{def}}{=}\bar{\alpha}$).

The definitions of the plastic velocity gradient $\overline{\boldsymbol{L}}^{p}$ and strain-like ISV then follow as

$$\overline{C}^{e}_{\bar{L}\bar{B}}\overline{L}^{p\bar{B}}_{\cdot\bar{K}}\overset{\text{def}}{=}\dot{\bar{\gamma}}\frac{\partial\overline{F}}{\partial\overline{S}^{\bar{K}\bar{L}}} \tag{70}$$

$$\frac{\partial\overline{F}}{\partial\overline{S}^{\bar{K}\bar{L}}}=\overline{G}_{\bar{K}\bar{A}}\widehat{\overline{N}}^{\bar{A}\bar{B}}\overline{G}_{\bar{B}\bar{L}}$$

$$\widehat{\overline{N}}^{\bar{A}\bar{B}}=\frac{\text{dev}\overline{S}^{\bar{A}\bar{B}}}{\left\|\text{dev}\overline{\boldsymbol{S}}\right\|}$$

$$\dot{\overline{Z}}\overset{\text{def}}{=}-\dot{\bar{\gamma}}\frac{\partial\overline{F}}{\partial\bar{\alpha}}=\dot{\bar{\gamma}} \tag{71}$$

$$\bar{\alpha}=\overline{H}\overline{Z} \tag{72}$$

where $\dot{\bar{\gamma}}$ is the macro-plastic multiplier.

7.2.2. Micro-scale plasticity

For micro-scale plasticity, we write the yield function $\overline{F}^{\chi}$ as

$$\overline{F}^{\chi}\left(\overline{\boldsymbol{\Sigma}}-\overline{\boldsymbol{S}},\bar{\alpha}^{\chi}\right)\overset{\text{def}}{=}\left\|\text{dev}\left(\overline{\boldsymbol{\Sigma}}-\overline{\boldsymbol{S}}\right)\right\|-\bar{\alpha}^{\chi}\leqslant 0 \tag{73}$$

$$\text{dev}\left(\overline{\Sigma}^{\bar{I}\bar{J}}-\overline{S}^{\bar{I}\bar{J}}\right)=\left(\overline{\Sigma}^{\bar{I}\bar{J}}-\overline{S}^{\bar{I}\bar{J}}\right)-\left[\frac{1}{3}\overline{C}^{e}_{\bar{A}\bar{B}}\left(\overline{\Sigma}^{\bar{A}\bar{B}}-\overline{S}^{\bar{A}\bar{B}}\right)\right]\left(\overline{C}^{e-1}\right)^{\bar{I}\bar{J}}$$

where $\bar{\alpha}^{\chi}$ is the micro-yield strength (stress-like ISV $\overline{Q}^{\chi}\overset{\text{def}}{=}\bar{\alpha}^{\chi}$). Note that at the micro-scale, the yield strength can be determined separately from the macro-scale parameter $\bar{\alpha}$.

Remark 2. We use the same functional forms for macro- and micro-plasticity ($\overline{F}^{\chi}$ with similar functional form as $\overline{F}$, but different ISVs and parameters), but this is only for the example model presented here. It is possible for the functional forms to be different when representing different phenomenology at the micro- and macro-scales. More micromechanical analysis and experimental data are necessary to determine the micro-plasticity functional forms in the future.

The definitions of the micro-scale plastic velocity gradient $\overline{\boldsymbol{L}}^{\chi,p}$ and strain-like ISV then follow as

$$\overline{\Psi}^{e}_{\bar{L}\bar{E}}\overline{L}^{\chi,p\bar{E}}_{\cdot\bar{F}}\left(\overline{C}^{\chi,e-1}\right)^{\overline{FN}}\overline{\Psi}^{e}_{\bar{K}\bar{N}}\overset{\text{def}}{=}\dot{\bar{\gamma}}^{\chi}\frac{\partial\overline{F}^{\chi}}{\partial\left(\overline{\Sigma}^{\bar{K}\bar{L}}-\overline{S}^{\bar{K}\bar{L}}\right)} \tag{74}$$

$$\frac{\partial\overline{F}^{\chi}}{\partial\left(\overline{\Sigma}^{\bar{K}\bar{L}}-\overline{S}^{\bar{K}\bar{L}}\right)}=\overline{G}_{\bar{K}\bar{A}}\widehat{\overline{N}}^{\chi\bar{A}\bar{B}}\overline{G}_{\bar{B}\bar{L}}$$

$$\widehat{\overline{N}}^{\chi\bar{A}\bar{B}}=\frac{\text{dev}\left(\overline{\Sigma}^{\bar{A}\bar{B}}-\overline{S}^{\bar{A}\bar{B}}\right)}{\left\|\text{dev}\left(\overline{\boldsymbol{\Sigma}}-\overline{\boldsymbol{S}}\right)\right\|}$$

$$\dot{\overline{Z}}^{\chi}\overset{\text{def}}{=}-\dot{\bar{\gamma}}^{\chi}\frac{\partial\overline{F}^{\chi}}{\partial\bar{\alpha}^{\chi}}=\dot{\bar{\gamma}}^{\chi} \tag{75}$$

$$\bar{\alpha}^{\chi}=\overline{H}^{\chi}\overline{Z}^{\chi} \tag{76}$$

where $\dot{\bar{\gamma}}^{\chi}$ is the micro-plastic multiplier.

7.2.3. Micro-scale gradient plasticity

For micro-scale gradient plasticity, we write the yield function $\overline{F}^{\nabla\chi}$ as

$$\overline{F}^{\nabla\chi}\left(\overline{\boldsymbol{M}},\bar{\boldsymbol{\alpha}}^{\nabla\chi}\right)\overset{\text{def}}{=}\left\|\text{dev}\overline{\boldsymbol{M}}\right\|-\left\|\bar{\boldsymbol{\alpha}}^{\nabla\chi}\right\|\leqslant 0 \tag{77}$$

$$\text{dev}\overline{M}^{\bar{I}\bar{J}\bar{K}}=\overline{M}^{\bar{I}\bar{J}\bar{K}}-\left(\overline{C}^{e-1}\right)^{\bar{I}\bar{J}}\left[\frac{1}{3}\overline{C}^{e}_{\bar{A}\bar{B}}\overline{M}^{\bar{A}\bar{B}\bar{K}}\right]$$

where $\bar{\boldsymbol{\alpha}}^{\nabla\chi}$ is the micro-gradient yield strength (stress-like ISV $\overline{\boldsymbol{Q}}^{\nabla\chi}\overset{\text{def}}{=}\bar{\boldsymbol{\alpha}}^{\nabla\chi}$). Note that at the gradient micro-scale, the yield strength can be determined separately from the micro- and macro-scale parameters, which is a constitutive assumption. The definitions of the covariant derivative of micro-scale plastic velocity gradient $\bar{\nabla}\overline{\boldsymbol{L}}^{\chi,p}$ and strain-like ISV then follow as

$$\overline{\Psi}^{e}_{\bar{L}\bar{D}}\overline{L}^{\chi,p\bar{D}}_{\bar{M},\bar{K}}-2\overline{\Psi}^{e}_{\bar{L}\bar{D}}\text{skw}\left[\overline{L}^{\chi,p\bar{D}}_{\bar{C}}\left(\overline{\Psi}^{e-1}\right)^{\bar{C}\bar{F}}\overline{\Gamma}^{e}_{\bar{F}\bar{M}\bar{K}}\right]\overset{\text{def}}{=}\dot{\bar{\gamma}}^{\nabla\chi}\frac{\partial\overline{F}^{\nabla\chi}}{\partial\overline{M}^{\bar{K}\bar{L}\bar{M}}} \tag{78}$$

$$\frac{\partial\overline{F}^{\nabla\chi}}{\partial\overline{M}^{\bar{K}\bar{L}\bar{M}}}=\frac{\text{dev}\overline{M}^{\bar{P}\bar{I}\bar{J}}}{\left\|\text{dev}\overline{\boldsymbol{M}}\right\|}\overline{G}_{\bar{P}\bar{K}}\overline{G}_{\bar{I}\bar{L}}\overline{G}_{\bar{J}\bar{M}}$$

$$\frac{D\left(\overline{Z}^{\chi}_{\cdot\bar{A}}\right)}{Dt}\overset{\text{def}}{=}-\dot{\bar{\gamma}}^{\nabla\chi}\frac{\partial\overline{F}^{\nabla\chi}}{\partial\bar{\alpha}^{\nabla\chi,\bar{A}}}=\left(\dot{\bar{\gamma}}^{\nabla\chi}\right)\frac{\bar{\alpha}^{\nabla\chi,\bar{B}}}{\left\|\bar{\boldsymbol{\alpha}}^{\nabla\chi}\right\|}\overline{G}_{\bar{B}\bar{A}} \tag{79}$$

$$\bar{\alpha}^{\nabla\chi,\bar{L}}=\overline{H}^{\nabla\chi}\overline{Z}^{\chi}_{\cdot\bar{A}}\overline{G}^{\bar{A}\bar{L}} \tag{80}$$

where $\dot{\bar{\gamma}}^{\nabla\chi}$ is the micro-plastic gradient multiplier.

Remark 3. The main advantage to defining constitutively the evolution of the covariant derivative of micro-scale plastic velocity gradient $\bar{\nabla}\overline{\boldsymbol{L}}^{\chi,p}$ in (78) separate from the micro-scale plastic velocity gradient $\overline{\boldsymbol{L}}^{\chi,p}$ in (74) (i.e., no PDE in $\dot{\chi}^{p\bar{K}}_{\cdot\bar{K}}$) is to avoid finite element solution of an additional balance equation in weak form. One could allow $\bar{\nabla}\overline{\boldsymbol{L}}^{\chi,p}$ and $\bar{\nabla}\dot{\overline{Z}}^{\chi}$ to be defined as the covariant derivatives of $\overline{\boldsymbol{L}}^{\chi,p}$ and $\dot{\overline{Z}}^{\chi}$, respectively, but then the plastic evolution equations are PDEs and require coupled finite element implementation (such as in Regueiro et al. (2007)). We plan to implement the model, after time integration in Section 8, within a coupled finite element formulation for the coupled balance of linear and first moment of momentum, and thus avoiding another coupled equation to include in the finite element equations is desired. We will assess the accuracy of calculating $\bar{\nabla}\boldsymbol{\chi}^{p}$ by this direct time integration. Further discussion is provided in Section 9 for an anti-plane shear version of the model.

Remark 4. With these evolution equations in $\overline{\mathscr{B}}$, (70) can be integrated numerically to solve for $\boldsymbol{F}^{p}$ and in turn $\boldsymbol{F}^{e}$, (74) can be integrated numerically to solve for $\boldsymbol{\chi}^{p}$ and in turn $\boldsymbol{\chi}^{e}$, and (78) can be integrated numerically to solve for $\bar{\nabla}\boldsymbol{\chi}^{p}$ and in turn $\bar{\nabla}\boldsymbol{\chi}^{e}$. Then, the stresses $\overline{\boldsymbol{S}}$, $\overline{\boldsymbol{\Sigma}}-\overline{\boldsymbol{S}}$, and $\overline{\boldsymbol{M}}$ can be calculated and mapped to the current configuration to update the balance equations for finite element nonlinear solution. Such numerical time integration will be carried out in Section 8, and finite element implementation is ongoing work.

8. Numerical time integration

The constitutive equations in Section 7 are integrated numerically in time following a semi-implicit scheme (Moran et al., 1990). The advantage of such a scheme is the simplicity for integrating complex constitutive models while maintaining frame indifference of the integration. The disadvantage is that it is conditionally stable and thus care must be taken in choosing a stable time step. We will solve for plastic multiplier increments $\Delta\bar{\gamma}$ and $\Delta\bar{\gamma}^{\chi}$ in a coupled fashion (if yielding is detected at both scales; see Box 3), and multiplier $\Delta\bar{\gamma}^{\nabla\chi}$ afterward because it is uncoupled. The plastic multipliers $\Delta\bar{\gamma}$ and $\Delta\bar{\gamma}^{\chi}$ are uncoupled from $\Delta\bar{\gamma}^{\nabla\chi}$ because of the assumption of small elastic deformations and dropping the quadratic terms in (60) and (61).

We assume a deformation-driven time integration scheme within a coupled finite element program solving the isothermal coupled

balance of linear momentum and first moment of momentum equations (17) and (18), respectively, such that deformation gradient $\boldsymbol{F}_{n+1}$ and micro-deformation tensor $\boldsymbol{\chi}_{n+1}$ are given at time t_{n+1}, as well as their increments $\Delta\boldsymbol{F}_{n+1} = \boldsymbol{F}_{n+1} - \boldsymbol{F}_n$ and $\Delta\boldsymbol{\chi}_{n+1} = \boldsymbol{\chi}_{n+1} - \boldsymbol{\chi}_n$. We assume a time step $\Delta t = t_{n+1} - t_n$. Boxes 1-2 provide summaries of the semi-implicit time integration of the stress and plastic evolution equations, respectively, in symbolic form. For $\nabla_X\boldsymbol{\chi}_{n+1}$ in Box 2, because $\boldsymbol{\Phi}$ is a nodal degree of freedom in a finite element solution and thus interpolated in a standard fashion, its spatial gradient can be calculated.

Box 3 summarizes the algorithm for solving the plastic multipliers from evaluating the yield functions at time t_{n+1}. It involves multiple plastic yield checks, such that macro- and/or micro-plasticity could be enabled, and/or micro-gradient plasticity. Because the macro- and micro-plasticity yield functions $\bar{F}$ and $\bar{F}^{\chi}$, respectively, are decoupled from the micro-gradient plastic multiplier $\dot{\bar{\gamma}}^{\nabla\chi}$, we will solve first for the micro- and macro-plastic multipliers, as indicated by (I) in Box 3, and then for the micro-gradient plastic multiplier in (II) afterward. Once the plastic multipliers are calculated, the stresses and ISVs can be updated as indicated in Boxes 1-2.

Box 1
Semi-implicit numerical integration of macro- and micro-plastic evolution equations.

Given: $\boldsymbol{F}_{n+1}, \boldsymbol{\chi}_{n+1}, \bar{\boldsymbol{C}}^e_n, \bar{\boldsymbol{\Psi}}^e_n, \boldsymbol{F}^p_n, \boldsymbol{\chi}^p_n, \bar{Z}_n, \bar{Z}^{\chi}_n, \bar{\alpha}_n, \bar{\alpha}^{\chi}_n$

1. Calculate trial values and yield functions:

$$\boldsymbol{F}^{e\mathrm{tr}} = \boldsymbol{F}_{n+1}\boldsymbol{F}^{p-1}_n$$
$$\bar{\boldsymbol{C}}^{e\mathrm{tr}} = \boldsymbol{F}^{e\mathrm{tr}T}\boldsymbol{F}^{e\mathrm{tr}}$$
$$\bar{\boldsymbol{E}}^{e\mathrm{tr}} = \left(\bar{\boldsymbol{C}}^{e\mathrm{tr}} - \bar{\boldsymbol{1}}\right)/2$$
$$\boldsymbol{\chi}^{e\mathrm{tr}} = \boldsymbol{\chi}_{n+1}\boldsymbol{\chi}^{p-1}_n$$
$$\bar{\boldsymbol{\Psi}}^{e\mathrm{tr}} = \boldsymbol{F}^{e\mathrm{tr}T}\boldsymbol{\chi}^{e\mathrm{tr}}$$
$$\bar{\mathscr{E}}^{e\mathrm{tr}} = \bar{\boldsymbol{\Psi}}^{e\mathrm{tr}} - \bar{\boldsymbol{1}}$$
$$\bar{\boldsymbol{S}}^{\mathrm{tr}} = \left(\bar{\boldsymbol{A}} + \bar{\boldsymbol{D}}\right) : \bar{\boldsymbol{E}}^{e\mathrm{tr}} + (\bar{\boldsymbol{B}} + \bar{\boldsymbol{D}}) : \bar{\mathscr{E}}^{e\mathrm{tr}}$$
$$\left(\bar{\boldsymbol{\Sigma}} - \bar{\boldsymbol{S}}\right)^{\mathrm{tr}} = \tau(tr\bar{\boldsymbol{E}}^{e_{\mathrm{tr}}})\bar{\boldsymbol{1}} + (\eta - \tau)(tr\bar{\mathscr{E}}^{e_{\mathrm{tr}}})\bar{\boldsymbol{1}} + 2\sigma(\bar{\boldsymbol{E}}^{e_{\mathrm{tr}}}) + (\nu - \tau)\bar{\mathscr{E}}^{e_{\mathrm{tr}}} + (\kappa - \sigma)\bar{\mathscr{E}}^{eT\mathrm{tr}}$$
$$\bar{F}^{\mathrm{tr}} = \bar{F}\left(\bar{\boldsymbol{S}}^{\mathrm{tr}}, \bar{\boldsymbol{C}}^{e\mathrm{tr}}, \bar{\alpha}_n\right)$$
$$\bar{F}^{\chi,\mathrm{tr}} = \bar{F}^{\chi}\left(\left(\bar{\boldsymbol{\Sigma}} - \bar{\boldsymbol{S}}\right)^{\mathrm{tr}}, \bar{\boldsymbol{C}}^{e\mathrm{tr}}, \bar{\alpha}^{\chi}_n\right)$$

2. Integrate plastic part of deformation gradient $\boldsymbol{F}^p_{n+1}$ and micro-deformation tensor $\boldsymbol{\chi}^p_{n+1}$:

$$\bar{\boldsymbol{C}}^e_n\dot{\bar{\boldsymbol{F}}}^p_{n+1}\boldsymbol{F}^{p-1}_n = \dot{\bar{\gamma}}_{n+1}\frac{\partial\bar{F}}{\partial\bar{\boldsymbol{S}}^{\mathrm{tr}_T}}$$
$$\boldsymbol{F}^p_{n+1} = \left[\bar{\boldsymbol{1}} + \Delta\bar{\gamma}_{n+1}\bar{\boldsymbol{C}}^{e-1}_n\frac{\partial\bar{F}}{\partial\bar{\boldsymbol{S}}^{\mathrm{tr}T}}\right]\boldsymbol{F}^p_n$$
$$\bar{\boldsymbol{\Psi}}^e_n\dot{\boldsymbol{\chi}}^p_{n+1}\boldsymbol{\chi}^{p-1}_n\bar{\boldsymbol{C}}^{\chi,e-1}_n\bar{\boldsymbol{\Psi}}^{eT}_n = \dot{\bar{\gamma}}^{\chi}_{n+1}\frac{\partial\bar{F}^{\chi}}{\partial\left(\bar{\boldsymbol{\Sigma}} - \bar{\boldsymbol{S}}\right)^{\mathrm{tr}^T}}$$
$$\boldsymbol{\chi}^p_{n+1} = \left[\bar{\boldsymbol{1}} + \Delta\bar{\gamma}^{\chi}_{n+1}\bar{\boldsymbol{\Psi}}^{e-1}_n\frac{\partial\bar{F}^{\chi}}{\partial\left(\bar{\boldsymbol{\Sigma}} - \bar{\boldsymbol{S}}\right)^{\mathrm{tr}^T}}\bar{\boldsymbol{\Psi}}^{e-T}_n\bar{\boldsymbol{C}}^{\chi,e}_n\right]\boldsymbol{\chi}^p_n$$

3. Update elastic deformation:

$$\boldsymbol{F}^e_{n+1} = \boldsymbol{F}_{n+1}\boldsymbol{F}^{p-1}_{n+1}, \quad \bar{\boldsymbol{C}}^e_{n+1} = \boldsymbol{F}^{eT}_{n+1}\boldsymbol{F}^e_{n+1}, \quad \bar{\boldsymbol{E}}^e_{n+1} = \left(\bar{\boldsymbol{C}}^e_{n+1} - \bar{\boldsymbol{1}}\right)/2$$
$$\boldsymbol{\chi}^e_{n+1} = \boldsymbol{\chi}_{n+1}\boldsymbol{\chi}^{p-1}_{n+1}, \quad \bar{\boldsymbol{\Psi}}^e_{n+1} = \boldsymbol{F}^{eT}_{n+1}\boldsymbol{\chi}^e_{n+1}, \quad \bar{\mathscr{E}}^e_{n+1} = \bar{\boldsymbol{\Psi}}^e_{n+1} - \bar{\boldsymbol{1}}$$

4. Update stresses:

$$\bar{\boldsymbol{S}}_{n+1} = \left(\bar{\boldsymbol{A}} + \bar{\boldsymbol{D}}\right) : \bar{\boldsymbol{E}}^e_{n+1} + (\bar{\boldsymbol{B}} + \bar{\boldsymbol{D}}) : \bar{\mathscr{E}}^e_{n+1}$$
$$\left(\bar{\boldsymbol{\Sigma}} - \bar{\boldsymbol{S}}\right)_{n+1} = \tau(tr\bar{\boldsymbol{E}}^e_{n+1})\bar{\boldsymbol{1}} + (\eta - \tau)(tr\bar{\mathscr{E}}^e_{n+1})\bar{\boldsymbol{1}} + 2\sigma(\bar{\boldsymbol{E}}^e_{n+1})\bar{\boldsymbol{1}} + (\nu - \sigma)\bar{\mathscr{E}}^e_{n+1} + (\kappa - \sigma)\bar{\mathscr{E}}^{eT}_{n+1}$$

5. Integrate strain-like ISVs, and update stress-like ISVs:

$$\bar{Z}_{n+1} = \bar{Z}_n + \Delta\bar{\gamma}_{n+1}, \quad \bar{\alpha}_{n+1} = \bar{H}\bar{Z}_{n+1}$$
$$\bar{Z}^{\chi}_{n+1} = \bar{Z}^{\chi}_n + \Delta\bar{\gamma}^{\chi}_{n+1}, \quad \bar{\alpha}^{\chi}_{n+1} = \bar{H}^{\chi}\bar{Z}^{\chi}_{n+1}$$

6. Solve for $\Delta\bar{\gamma}_{n+1}$ and $\Delta\bar{\gamma}^{\chi}_{n+1}$ using Newton–Raphson in Box 3.

Box 2
Semi-implicit numerical integration of micro-gradient plastic evolution equations.

Given: $\nabla_X\boldsymbol{\chi}_{n+1}, \boldsymbol{F}^e_{n+1}, \bar{\boldsymbol{C}}^e_{n+1}, \boldsymbol{\chi}^e_{n+1}, \bar{\boldsymbol{\Psi}}^e_{n+1}, \boldsymbol{F}^p_{n+1}, \quad \boldsymbol{F}^p_n, \boldsymbol{\chi}^p_{n+1}, \boldsymbol{\chi}^p_n, \left(\bar{\nabla}\boldsymbol{\chi}^p\right)_n, \left(\bar{\nabla}\bar{Z}^{\chi}\right)_n, \bar{\boldsymbol{\alpha}}^{\nabla\chi}_n$

1. Calculate trial values and yield function: Using $(\bullet)_{\cdot\bar{K}} \overset{\mathrm{def}}{=} (\bullet)_{\cdot K}F^{p-1K}_{\cdot\bar{K}}$

$$\bar{\nabla}\boldsymbol{\chi}^e = \left[(\nabla_X\boldsymbol{\chi})\boldsymbol{F}^{p-1} - \boldsymbol{\chi}^e\left(\bar{\nabla}\boldsymbol{\chi}^p\right)\right] \odot \boldsymbol{\chi}^{p-1}$$

then

$$\left(\bar{\nabla}\boldsymbol{\chi}\right)^{e\mathrm{tr}} = \left[(\nabla_X\boldsymbol{\chi}_{n+1})\boldsymbol{F}^{p-1}_{n+1} - \boldsymbol{\chi}^e_{n+1}\left(\bar{\nabla}\boldsymbol{\chi}^p\right)_n\right] \odot \boldsymbol{\chi}^{p-1}_{n+1}$$
$$\boldsymbol{\Gamma}^{e\mathrm{tr}} = \boldsymbol{F}^{eT}_{n+1}\left(\bar{\nabla}\boldsymbol{\chi}\right)^{e\mathrm{tr}}$$
$$\bar{\boldsymbol{M}}^{\mathrm{tr}} = \bar{\boldsymbol{C}} : \boldsymbol{\Gamma}^{e\mathrm{tr}}$$
$$\bar{F}^{\nabla\chi,\mathrm{tr}} = \bar{F}^{\nabla\chi}\left(\bar{\boldsymbol{M}}^{\mathrm{tr}}, \bar{\boldsymbol{\alpha}}^{\nabla\chi}_n\right)$$

2. Integrate micro-plastic gradient tensor $\bar{\nabla}\boldsymbol{\chi}^p_{n+1}$: First, from Eq. (47),

$$\bar{\nabla}\bar{\boldsymbol{L}}^{\chi,p} = \left[\bar{\nabla}\dot{\boldsymbol{\chi}}^p - \bar{\boldsymbol{L}}^{\chi,p}\left(\bar{\nabla}\boldsymbol{\chi}^p\right)\right] \odot \boldsymbol{\chi}^{p-1}$$

where it can be shown that $\bar{\nabla}\dot{\boldsymbol{\chi}}^p = D\left(\bar{\nabla}\boldsymbol{\chi}^p\right)/Dt + \left(\bar{\nabla}\boldsymbol{\chi}^p\right)\bar{\boldsymbol{L}}^p$. Second, recall from Eq. (78),

$$\bar{\nabla}\bar{\boldsymbol{L}}^{\chi,p} = \left(\dot{\bar{\gamma}}^{\nabla\chi}\right)\bar{\boldsymbol{\Psi}}^{e-1}_n \odot \frac{\partial\bar{F}^{\nabla\chi}}{\partial\bar{\boldsymbol{M}}^T} + 2\mathrm{skw}\left[\bar{\boldsymbol{L}}^{\chi,p}\bar{\boldsymbol{\Psi}}^{e-1}\bar{\boldsymbol{\Gamma}}^e\right]$$

Third, set the previous two equations equal to each other to come up with an evolution equation for $\bar{\nabla}\boldsymbol{\chi}^p$ as

$$\frac{D\left(\bar{\nabla}\boldsymbol{\chi}^p\right)}{Dt} = \left(\dot{\bar{\gamma}}^{\nabla\chi}\right)\bar{\boldsymbol{\Psi}}^{e-1} \odot \frac{\partial\bar{F}^{\nabla\chi}}{\partial\bar{\boldsymbol{M}}^T} \odot \boldsymbol{\chi}^p + 2\mathrm{skw}\left[\bar{\boldsymbol{L}}^{\chi,p}\bar{\boldsymbol{\Psi}}^{e-1}\bar{\boldsymbol{\Gamma}}^e\right] \odot \boldsymbol{\chi}^p - \left(\bar{\nabla}\boldsymbol{\chi}^p\right)\bar{\boldsymbol{L}}^p + \bar{\boldsymbol{L}}^{\chi,p}\left(\bar{\nabla}\boldsymbol{\chi}^p\right)$$

Then, the semi-implicit time integration is written as

$$\left(\bar{\nabla}\boldsymbol{\chi}^p\right)_{n+1} = \left(\bar{\nabla}\boldsymbol{\chi}^p\right)_n + \left(\Delta\bar{\gamma}^{\nabla\chi}_{n+1}\right)\bar{\boldsymbol{\Psi}}^{e-1}_{n+1} \odot \frac{\partial\bar{F}^{\nabla\chi}}{\partial\bar{\boldsymbol{M}}^{\mathrm{tr}T}} \odot \boldsymbol{\chi}^p_{n+1} + 2\mathrm{skw}\left[\Delta\bar{\boldsymbol{L}}^{\chi,p}_{n+1}\bar{\boldsymbol{\Psi}}^{e-1}_{n+1}\bar{\boldsymbol{\Gamma}}^e_n\right] \odot \boldsymbol{\chi}^p_{n+1} - \left(\bar{\nabla}\boldsymbol{\chi}^p\right)_n\left(\Delta\bar{\boldsymbol{L}}^p_{n+1}\right) + \left(\Delta\bar{\boldsymbol{L}}^{\chi,p}_{n+1}\right)\left(\bar{\nabla}\boldsymbol{\chi}^p\right)_n$$

where $\Delta\bar{\boldsymbol{L}}^p_{n+1} = (\Delta\boldsymbol{F}^p_{n+1})\boldsymbol{F}^{p-1}_{n+1}$ and $\Delta\bar{\boldsymbol{L}}^{\chi,p}_{n+1} = (\Delta\boldsymbol{\chi}^p_{n+1})\boldsymbol{\chi}^{p-1}_{n+1}$.

3. Update elastic deformation and stress:

$$\left(\bar{\mathbf{\nabla}}\boldsymbol{\chi}^e\right)_{n+1} = \left[\left(\mathbf{\nabla}_X\boldsymbol{\chi}_{n+1}\right)\boldsymbol{F}^{p-1}_{n+1} - \boldsymbol{\chi}^e_{n+1}\left(\bar{\mathbf{\nabla}}\boldsymbol{\chi}^p\right)_{n+1}\right] \odot \boldsymbol{\chi}^{p-1}_{n+1}$$

$$\boldsymbol{\Gamma}^e_{n+1} = \boldsymbol{F}^{eT}_{n+1}\left(\bar{\mathbf{\nabla}}\boldsymbol{\chi}^e\right)_{n+1}$$

$$\overline{\boldsymbol{M}}_{n+1} = \overline{\boldsymbol{C}}:\boldsymbol{\Gamma}^e_{n+1}$$

4. Integrate strain-like ISVs, and update stress-like ISVs:

$$\left(\bar{\mathbf{\nabla}}\overline{Z}^\chi\right)_{n+1} = \left(\bar{\mathbf{\nabla}}\overline{Z}^\chi\right)_n + \left(\Delta\bar{\gamma}^{\nabla\chi}_{n+1}\right)\left(\frac{\bar{\boldsymbol{\alpha}}^{\nabla\chi}_n}{\left\|\bar{\boldsymbol{\alpha}}^{\nabla\chi}_n\right\|}\right)\overline{\boldsymbol{C}}^e_{n+1}$$

$$\bar{\boldsymbol{\alpha}}^{\nabla\chi}_{n+1} = \overline{H}^{\nabla\chi}\left(\bar{\mathbf{\nabla}}\overline{Z}^\chi\right)_{n+1}\overline{\boldsymbol{C}}^{e-1}_{n+1}$$

5. Solve for $\Delta\bar{\gamma}^{\nabla\chi}_{n+1}$ using Newton–Raphson in Box 3.

Box 3
Check for plastic yielding and solve for plastic multipliers.

(I) Solve for macro- and micro-plastic multipliers $\Delta\bar{\gamma}$ and $\Delta\bar{\gamma}^\chi$:

Consider three cases:

(i) If $\overline{F}^{\mathrm{tr}} > 0$ and $\overline{F}^{\chi,\mathrm{tr}} > 0$, solve for $\Delta\bar{\gamma}_{n+1}$ and $\Delta\bar{\gamma}^\chi_{n+1}$ using Newton–Raphson on coupled equations:

$$\overline{F}\left(\overline{\boldsymbol{S}}_{n+1}, \overline{\boldsymbol{C}}^e_{n+1}, \bar{\alpha}_{n+1}\right) = \overline{F}\left(\Delta\bar{\gamma}_{n+1}, \Delta\bar{\gamma}^\chi_{n+1}\right) = 0$$

$$\overline{F}^\chi\left(\left(\overline{\boldsymbol{\Sigma}} - \overline{\boldsymbol{S}}\right)_{n+1}, \overline{\boldsymbol{C}}^e_{n+1}, \bar{\alpha}^\chi_{n+1}\right) = \overline{F}^\chi\left(\Delta\bar{\gamma}_{n+1}, \Delta\bar{\gamma}^\chi_{n+1}\right) = 0$$

(ii) If $\overline{F}^{\mathrm{tr}} > 0$ and $\overline{F}^{\chi,\mathrm{tr}} < 0$, solve for $\Delta\bar{\gamma}_{n+1}$ with $\Delta\bar{\gamma}^\chi_{n+1} = 0$ using Newton–Raphson:

$$\overline{F}\left(\overline{\boldsymbol{S}}_{n+1}, \overline{\boldsymbol{C}}^e_{n+1}, \bar{\alpha}_{n+1}\right) = \overline{F}\left(\Delta\bar{\gamma}_{n+1}, \Delta\bar{\gamma}^\chi_{n+1} = 0\right) = 0$$

(iii) If $\overline{F}^{\mathrm{tr}} < 0$ and $\overline{F}^{\chi,\mathrm{tr}} > 0$, solve for $\Delta\bar{\gamma}^\chi_{n+1}$ with $\Delta\bar{\gamma}_{n+1} = 0$ using Newton–Raphson:

$$\overline{F}^\chi\left(\left(\overline{\boldsymbol{\Sigma}} - \overline{\boldsymbol{S}}\right)_{n+1}, \overline{\boldsymbol{C}}^e_{n+1}, \bar{\alpha}^\chi_{n+1}\right) = \overline{F}^\chi\left(\Delta\bar{\gamma}_{n+1} = 0, \Delta\bar{\gamma}^\chi_{n+1}\right) = 0$$

(II) Solve for micro-gradient plastic multiplier $\Delta\bar{\gamma}^{\nabla\chi}$, given $\Delta\bar{\gamma}$ and $\Delta\bar{\gamma}^\chi$:

If $\overline{F}^{\nabla\chi,\mathrm{tr}} > 0$, solve for $\Delta\bar{\gamma}^{\nabla\chi}_{n+1}$ using Newton–Raphson:

$$\overline{F}^{\nabla\chi}\left(\overline{\boldsymbol{M}}_{n+1}, \bar{\boldsymbol{\alpha}}^{\nabla\chi}_{n+1}\right) = \overline{F}^{\nabla\chi}\left(\Delta\bar{\gamma}^{\nabla\chi}_{n+1}\right) = 0$$

This micromorphic elastoplasticity model numerical integration scheme will fit into a coupled Lagrangian finite element formulation and implementation of the balance of linear momentum and first moment of momentum. Such work is ongoing.

9. Anti-plane shear model

To present a simpler version of the general three-dimensional model discussed up to this point, we consider a strict anti-plane shear elasto-plasticity model in the context of micromorphic constitutive modeling presented in this paper. Such model is useful to better understand the finite element implementation, since it is easier to implement, but is limited physically to an unrealistic material. For example, for a single shear plane, the material will look like a deck of cards being sheared as in Fig. 4. Details of such model for a different elasto-plasticity model, and coupled nonlinear finite element formulation, are presented in Regueiro et al. (2007). The micromorphic model presented here can be implemented in a similar manner as described in Regueiro et al. (2007), although with an additional balance of first moment of momentum equation, and different constitutive equations. We assume a Cartesian coordinate system for all configurations (reference, intermediate, and current). The deformation for anti-plane shear is given through the current coordinates

$$\begin{aligned} x_1 &= X_1 \\ x_2 &= X_2 \\ x_3 &= X_3 + u(x_1, x_2) \end{aligned} \tag{81}$$

where x_i are the current coordinates, X_I are the reference coordinates, and $u(x_1, x_2)$ is the out-of-plane shear displacement. Thus, the problem reduces to a two-dimensional domain. The deformation gradient and micro-deformation tensor are then written as

$$\boldsymbol{F} = \frac{\partial \boldsymbol{x}}{\partial \boldsymbol{X}} = \mathbf{1} + \boldsymbol{s}\otimes\boldsymbol{\gamma}; \quad \boldsymbol{s}\cdot\boldsymbol{\gamma} = 0 \tag{82}$$

$$\boldsymbol{\gamma} = \frac{\partial u}{\partial \boldsymbol{X}} = \begin{bmatrix} \partial u/\partial X_1 \\ \partial u/\partial X_2 \\ 0 \end{bmatrix}; \qquad \boldsymbol{s} = \begin{bmatrix} 0 \\ 0 \\ 1 \end{bmatrix} \tag{83}$$

$$\boldsymbol{\chi} = \mathbf{1} + \boldsymbol{s}\otimes\boldsymbol{\phi}; \quad \boldsymbol{s}\cdot\boldsymbol{\phi} = 0, \quad \boldsymbol{\phi} = [\,\phi_1 \quad \phi_2 \quad 0\,]^T \tag{84}$$

where $\boldsymbol{\gamma}$ is the displacement gradient vector, $\boldsymbol{s}$ the out-of-plane normal and direction of shear displacement, and $\boldsymbol{\phi}$ the micro-displacement gradient vector. Note that $\partial u/\partial \boldsymbol{X} = \partial u/\partial \boldsymbol{x}$.

The anti-plane shear kinematics are *strict* (Cermelli and Gurtin, 2001) since we assume $\boldsymbol{F}^e$, $\boldsymbol{F}^p$, $\boldsymbol{\chi}^e$, and $\boldsymbol{\chi}^p$ take the same form as $\boldsymbol{F}$ and $\boldsymbol{\chi}$, such that

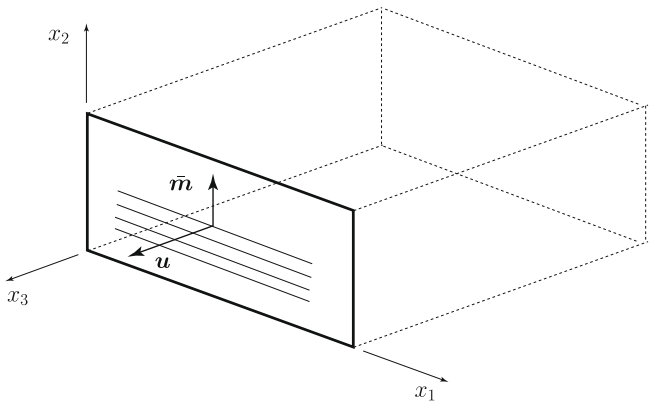

Fig. 4. Strict anti-plane shear for single slip with unit normal $\bar{\boldsymbol{m}}$ and displacement $\boldsymbol{u} = u(x_1, x_2)\boldsymbol{s}$, where $\boldsymbol{s} = \boldsymbol{e}_3$, similar to shearing a deck of playing cards.

$$\begin{aligned}
&\boldsymbol{F}^e := \boldsymbol{1} + \boldsymbol{s}\otimes\boldsymbol{\gamma}^e; \quad \boldsymbol{s}\cdot\boldsymbol{\gamma}^e = 0\\
&\boldsymbol{F}^p := \boldsymbol{1} + \boldsymbol{s}\otimes\boldsymbol{\gamma}^p; \quad \boldsymbol{s}\cdot\boldsymbol{\gamma}^p = 0\\
&\boldsymbol{\gamma} := \boldsymbol{\gamma}^e + \boldsymbol{\gamma}^p\\
&\boldsymbol{\gamma}^e = [\,\gamma_1^e \quad \gamma_2^e \quad 0\,]^T; \qquad \boldsymbol{\gamma}^p = [\,\gamma_1^p \quad \gamma_2^p \quad 0\,]^T
\end{aligned} \tag{85}$$

$$\begin{aligned}
&\boldsymbol{\chi}^e := \boldsymbol{1} + \boldsymbol{s}\otimes\boldsymbol{\phi}^e; \quad \boldsymbol{s}\cdot\boldsymbol{\phi}^e = 0\\
&\boldsymbol{\chi}^p := \boldsymbol{1} + \boldsymbol{s}\otimes\boldsymbol{\phi}^p; \quad \boldsymbol{s}\cdot\boldsymbol{\phi}^p = 0\\
&\boldsymbol{\phi} := \boldsymbol{\phi}^e + \boldsymbol{\phi}^p\\
&\boldsymbol{\phi}^e = [\,\phi_1^e \quad \phi_2^e \quad 0\,]^T; \qquad \boldsymbol{\phi}^p = [\,\phi_1^p \quad \phi_2^p \quad 0\,]^T
\end{aligned} \tag{86}$$

where $\boldsymbol{\gamma}^e$ and $\boldsymbol{\gamma}^p$ are macro-elastic and plastic vectors, respectively, and $\boldsymbol{\phi}^e$ and $\boldsymbol{\phi}^p$ the micro-elastic and plastic vectors. Note that the inverses are

$$(\boldsymbol{F}^e)^{-1} = \boldsymbol{1} - \boldsymbol{s}\otimes\boldsymbol{\gamma}^e, \quad (\boldsymbol{F}^p)^{-1} = \boldsymbol{1} - \boldsymbol{s}\otimes\boldsymbol{\gamma}^p \tag{87}$$

$$(\boldsymbol{\chi}^e)^{-1} = \boldsymbol{1} - \boldsymbol{s}\otimes\boldsymbol{\phi}^e, \quad (\boldsymbol{\chi}^p)^{-1} = \boldsymbol{1} - \boldsymbol{s}\otimes\boldsymbol{\phi}^p \tag{88}$$

The elastic deformation tensors, and plastic velocity gradients in the intermediate configuration can then be derived from these previous equations. For elastic deformation, we can show that

$$\overline{\boldsymbol{C}}^e = \boldsymbol{F}^{eT}\boldsymbol{F}^e = \boldsymbol{1} + \boldsymbol{\gamma}^e\otimes\boldsymbol{s} + \boldsymbol{s}\otimes\boldsymbol{\gamma}^e \tag{89}$$

$$\overline{\boldsymbol{C}}^{\chi,e} = \boldsymbol{\chi}^{eT}\boldsymbol{\chi}^e = \boldsymbol{1} + \boldsymbol{\phi}^e\otimes\boldsymbol{s} + \boldsymbol{s}\otimes\boldsymbol{\phi}^e \tag{90}$$

$$\overline{\boldsymbol{\Psi}}^e = \boldsymbol{F}^{eT}\boldsymbol{\chi}^e = \boldsymbol{1} + \boldsymbol{\gamma}^e\otimes\boldsymbol{s} + \boldsymbol{s}\otimes\boldsymbol{\phi}^e \tag{91}$$

$$\overline{\boldsymbol{\Gamma}}^e = \boldsymbol{F}^{eT}\frac{\partial\boldsymbol{\chi}^e}{\partial\overline{\boldsymbol{X}}} = \boldsymbol{s}\otimes\frac{\partial\boldsymbol{\phi}^e}{\partial\boldsymbol{X}}, \quad \overline{\Gamma}^e_{\overline{K}\overline{L}\overline{M}} = s_{\overline{K}}\frac{\partial\phi^e_{\overline{L}}}{\partial X_{\overline{M}}} \tag{92}$$

$$\overline{\boldsymbol{E}}^e = \left(\overline{\boldsymbol{C}}^e - \boldsymbol{1}\right)\Big/2 = (\boldsymbol{\gamma}^e\otimes\boldsymbol{s} + \boldsymbol{s}\otimes\boldsymbol{\gamma}^e)/2 \tag{93}$$

$$\overline{\mathscr{E}}^e = \overline{\boldsymbol{\Psi}}^e - \boldsymbol{1} = \boldsymbol{\gamma}^e\otimes\boldsymbol{s} + \boldsymbol{s}\otimes\boldsymbol{\phi}^e \tag{94}$$

where since we assume elastic deformations are small ($\|\boldsymbol{\gamma}^e\| \ll \varepsilon$ and $\|\boldsymbol{\phi}^e\| \ll \varepsilon$; ε a small positive number), we ignore quadratic terms in $\boldsymbol{\gamma}^e$ and $\boldsymbol{\phi}^e$, and also can show that $\partial\boldsymbol{\phi}^e/\partial\overline{\boldsymbol{X}} \approx \partial\boldsymbol{\phi}^e/\partial\boldsymbol{X}$. The index notation for $\overline{\boldsymbol{\Gamma}}^e$ is useful when writing the higher order stress $\overline{\boldsymbol{M}}$ in (97). We loosely use subscripts $\overline{K}$ in the intermediate configuration $\overline{\mathscr{B}}$ on variables in the current configuration, such as $\boldsymbol{s}$, because coordinates are nearly the same given strict anti-plane shear kinematics and small strain elastic deformation assumption. The stresses can then be derived as

$$\begin{aligned}
\overline{\boldsymbol{S}} = {}&(\mu+\sigma)(\boldsymbol{\gamma}^e\otimes\boldsymbol{s} + \boldsymbol{s}\otimes\boldsymbol{\gamma}^e) + \kappa(\boldsymbol{\gamma}^e\otimes\boldsymbol{s} + \boldsymbol{s}\otimes\boldsymbol{\phi}^e)\\
&+ \nu(\boldsymbol{s}\otimes\boldsymbol{\gamma}^e + \boldsymbol{\phi}^e\otimes\boldsymbol{s})
\end{aligned} \tag{95}$$

$$\begin{aligned}
\overline{\boldsymbol{\Sigma}} - \overline{\boldsymbol{S}} = {}&\sigma(\boldsymbol{\gamma}^e\otimes\boldsymbol{s} + \boldsymbol{s}\otimes\boldsymbol{\gamma}^e) + (\kappa-\sigma)(\boldsymbol{\phi}^e\otimes\boldsymbol{s} + \boldsymbol{s}\otimes\boldsymbol{\gamma}^e)\\
&+ (\nu-\sigma)(\boldsymbol{\gamma}^e\otimes\boldsymbol{s} + \boldsymbol{s}\otimes\boldsymbol{\phi}^e)
\end{aligned} \tag{96}$$

$$\begin{aligned}
\overline{M}_{\overline{K}\overline{L}\overline{M}} = {}&\tau_1\delta_{\overline{K}\overline{L}}\overline{\Gamma}^e_{\overline{M}\overline{Q}\overline{Q}} + \tau_4\overline{\Gamma}^e_{\overline{K}\overline{Q}\overline{Q}}\delta_{\overline{L}\overline{M}} + \tau_7\overline{\Gamma}^e_{\overline{K}\overline{L}\overline{M}}\\
&+ \tau_8\left(\overline{\Gamma}^e_{\overline{M}\overline{K}\overline{L}} + \overline{\Gamma}^e_{\overline{L}\overline{M}\overline{K}}\right) + \tau_9\overline{\Gamma}^e_{\overline{K}\overline{M}\overline{L}} + \tau_{10}\overline{\Gamma}^e_{\overline{L}\overline{K}\overline{M}}\\
&+ \tau_{11}\overline{\Gamma}^e_{\overline{M}\overline{L}\overline{K}}
\end{aligned} \tag{97}$$

For plastic velocity gradients, we can show that

$$\overline{\boldsymbol{L}}^p = \dot{\boldsymbol{F}}^p(\boldsymbol{F}^p)^{-1} = (\boldsymbol{s}\otimes\dot{\boldsymbol{\gamma}}^p)(\boldsymbol{1} - \boldsymbol{s}\otimes\boldsymbol{\gamma}^p) = \boldsymbol{s}\otimes\dot{\boldsymbol{\gamma}}^p \tag{98}$$

$$\overline{\boldsymbol{L}}^{\chi,p} = \dot{\boldsymbol{\chi}}^p(\boldsymbol{\chi}^p)^{-1} = (\boldsymbol{s}\otimes\dot{\boldsymbol{\phi}}^p)(\boldsymbol{1} - \boldsymbol{s}\otimes\boldsymbol{\phi}^p) = \boldsymbol{s}\otimes\dot{\boldsymbol{\phi}}^p \tag{99}$$

$$\overline{\nabla}\overline{\boldsymbol{L}}^{\chi,p} - 2\mathrm{skw}\left(\overline{\boldsymbol{L}}^{\chi,p}\overline{\boldsymbol{\Psi}}^{e^{-1}}\overline{\boldsymbol{\Gamma}}^e\right) \approx \overline{\nabla}\overline{\boldsymbol{L}}^{\chi,p} = \boldsymbol{s}\otimes\frac{\partial\dot{\boldsymbol{\phi}}^p}{\partial\boldsymbol{X}} \tag{100}$$

where for the third equation, gradient of micro-scale plastic velocity gradient, we again used the assumption of small elastic deformation to ignore quadratic terms in $\boldsymbol{\gamma}^e$ and $\boldsymbol{\phi}^e$, or their multiples. In the evolution equations for plastic deformation, we use the Mandel form of the reduced dissipation inequality (45), and can show because of small elastic deformations that these Mandel stresses are

$$\overline{\boldsymbol{S}}\overline{\boldsymbol{C}}^e \approx \overline{\boldsymbol{S}}, \quad \overline{\boldsymbol{C}}^{\chi,e^{-1}}\overline{\boldsymbol{\Psi}}^{eT}\left(\overline{\boldsymbol{\Sigma}} - \overline{\boldsymbol{S}}\right)\overline{\boldsymbol{\Psi}}^e \approx \overline{\boldsymbol{\Sigma}} - \overline{\boldsymbol{S}}, \quad \overline{\boldsymbol{M}}\overline{\boldsymbol{\Psi}}^e \approx \overline{\boldsymbol{M}} \tag{101}$$

The plastic evolution equations assume a number of slip systems α with unit normal vector $\bar{\boldsymbol{m}}^\alpha$ in the plane. For macro-scale plasticity, the evolution equations are

$$\begin{aligned}
&\dot{\boldsymbol{\gamma}}^p = \sum_\alpha \dot{\gamma}^\alpha\bar{\boldsymbol{m}}^\alpha\\
&\dot{\gamma}^\alpha = \dot{\gamma}_0^\alpha\left[\frac{\langle\overline{S}^\alpha\rangle}{\overline{Q}^\alpha}\right]^m\\
&\overline{S}^\alpha = \overline{\boldsymbol{S}} : (\boldsymbol{s}\otimes\bar{\boldsymbol{m}}^\alpha) = [(\mu+\sigma+\nu)\boldsymbol{\gamma}^e + \kappa\boldsymbol{\phi}^e]\bar{\boldsymbol{m}}^\alpha\\
&\dot{\overline{Q}}^\alpha = \overline{H}\dot{\gamma}^\alpha
\end{aligned} \tag{102}$$

where $\langle\bullet\rangle$ is the Macauley bracket. For micro-scale plasticity, the evolution equations are

$$\begin{aligned}
&\dot{\boldsymbol{\phi}}^p = \sum_\alpha \dot{\gamma}^{\chi,\alpha}\bar{\boldsymbol{m}}^\alpha\\
&\dot{\gamma}^{\chi,\alpha} = \dot{\gamma}_0^{\chi,\alpha}\left[\frac{\left\langle\left(\overline{\Sigma} - \overline{S}\right)^\alpha\right\rangle}{\overline{Q}^{\chi,\alpha}}\right]^m\\
&\left(\overline{\Sigma} - \overline{S}\right)^\alpha = \left(\overline{\boldsymbol{\Sigma}} - \overline{\boldsymbol{S}}\right) : (\boldsymbol{s}\otimes\bar{\boldsymbol{m}}^\alpha) = [\kappa\boldsymbol{\gamma}^e + (\nu-\sigma)\boldsymbol{\phi}^e]\bar{\boldsymbol{m}}^\alpha\\
&\dot{\overline{Q}}^{\chi,\alpha} = \overline{H}^\chi\dot{\gamma}^{\chi,\alpha}
\end{aligned} \tag{103}$$

We need $\partial\dot{\boldsymbol{\phi}}^p/\partial\boldsymbol{X}$ in order to calculate $\partial\dot{\boldsymbol{\phi}}^e/\partial\boldsymbol{X} = \partial\dot{\boldsymbol{\phi}}/\partial\boldsymbol{X} - \partial\dot{\boldsymbol{\phi}}^p/\partial\boldsymbol{X}$, and in turn $\overline{\boldsymbol{M}}$. For micro-scale gradient plasticity, we have two choices, as mentioned in Remark 1, to solve for $\partial\dot{\boldsymbol{\phi}}^p/\partial\boldsymbol{X}$: (1) calculate $\partial\dot{\boldsymbol{\phi}}^p/\partial\boldsymbol{X}$ directly as a gradient of $\dot{\boldsymbol{\phi}}^p$, where $\boldsymbol{\phi}^p$ is treated as an additional nodal dof in the finite element implementation, or (2) define an evolution equation. These two choices are summarized as follows and will be considered in the finite element implementation for future work:

1. Direct calculation of gradient $\partial\dot{\boldsymbol{\phi}}^p/\partial\boldsymbol{X}$. This would require expressing the micro-scale plasticity equation in weak form for finite element solution (Regueiro et al., 2007):

$$\dot{\boldsymbol{\phi}}^p - \sum_\alpha \dot{\gamma}^{\chi,\alpha}\bar{\boldsymbol{m}}^\alpha = \boldsymbol{0} \tag{104}$$

In this case, there is no yield function $\overline{F}^{\nabla\chi}$ from which to solve for a micro-scale gradient plastic multiplier $\dot{\gamma}^{\nabla\chi,\alpha}$ for slip system α, nor a gradient stress-like ISV $\overline{\boldsymbol{Q}}^{\nabla\chi,\alpha}$ for which to evolve.

2. Separate evolution equation:

$$\begin{aligned}
&\frac{\partial\dot{\boldsymbol{\phi}}^p}{\partial\boldsymbol{X}} = \sum_\alpha \dot{\gamma}^{\nabla\chi,\alpha}\bar{\boldsymbol{m}}^\alpha\otimes\bar{\boldsymbol{n}}^\alpha\\
&\bar{\boldsymbol{n}}^\alpha = \bar{\boldsymbol{m}}^\alpha\frac{\partial\boldsymbol{\phi}/\partial\boldsymbol{X}}{\|\partial\boldsymbol{\phi}/\partial\boldsymbol{X}\|}\\
&\dot{\gamma}^{\nabla\chi,\alpha} = \dot{\gamma}_0^{\nabla\chi,\alpha}\left[\frac{\|\overline{\boldsymbol{M}}^\alpha\|}{\|\overline{\boldsymbol{Q}}^{\nabla\chi,\alpha}\|}\right]^m\\
&\overline{M}^\alpha_I = \overline{M}_{j\overline{K}I}s_j\bar{m}^\alpha_{\overline{K}}\\
&\dot{\overline{\boldsymbol{Q}}}^{\nabla\chi,\alpha} = \overline{H}^{\nabla\chi}\dot{\gamma}^{\nabla\chi,\alpha}\bar{\boldsymbol{n}}^\alpha
\end{aligned} \tag{105}$$

In this case, a separate micro-scale gradient plastic multiplier $\dot{\gamma}^{\nabla\chi,\alpha}$ for each slip system α is solved, and a gradient stress-like ISV $\overline{\boldsymbol{Q}}^{\nabla\chi,\alpha}$, to solve for $\partial\dot{\boldsymbol{\phi}}^p/\partial\boldsymbol{X}$ from an evolution equation (105).

The numerical time integration, and finite element implementation, of these constitutive equations will follow the procedure

described in Regueiro et al. (2007). An additional balance equation, the balance of first moment of momentum (18), will likewise be formulated for anti-plane shear and implemented by a coupled finite element method in future work.

10. Conclusions

The paper formulated finite strain micromorphic elastoplasticity based on a multiplicative decomposition of the deformation gradient $\boldsymbol{F}$ and micro-deformation tensor $\boldsymbol{\chi}$ in the sense of micromorphic continuum mechanics by Eringen (1999). The Clausius–Duhem inequality written in the intermediate configuration provided constitutive forms for the plastic evolution equations to solve uniquely for plastic deformations $\boldsymbol{F}^p$, $\boldsymbol{\chi}^p$, and $\bar{\nabla}\boldsymbol{\chi}^p$, and in turn their elastic counterparts and the stresses and internal state variables. The Clausius–Duhem inequality was written in two forms (Mandel stress and an alternate 'metric' form), and thus it becomes a constitutive modeler's choice which form to use. Either approach will solve for $\boldsymbol{F}^p$, $\boldsymbol{\chi}^p$, and $\bar{\nabla}\boldsymbol{\chi}^p$, but their solutions could be different depending on which form is used and the particular constitutive equations chosen for the heterogeneous material of interest. The additional plastic evolution equation for $\bar{\nabla}\boldsymbol{\chi}^p$ in (51) or (54) removes the need for an additional weak form equation for finite element solution of $\boldsymbol{\chi}^p$, but such assumption will be compared to a direct computation of $\bar{\nabla}\boldsymbol{\chi}^p$ from a finite element interpolation of $\boldsymbol{\chi}^p$. In the metric form, evolution equations for J_2 plasticity were assumed, and also linear isotropic elasticity. A semi-implicit time integration scheme in the intermediate configuration was presented for future coupled Lagrangian finite element implementation. Another paper (Regueiro, 2009) presents non-associative Drucker-Prager micromorphic elastoplasticity mapped to the current configuration with semi-implicit time integration. An anti-plane shear model is presented to demonstrate a simpler two-dimensional form to implement in the future by the finite element method.

Acknowledgements

The support of National Science Foundation Grant CMMI-0700648, Army Research Office Grant W911NF-09-1-0111, and the Army Research Laboratory is gratefully acknowledged. The author also acknowledges Dr. A.C. Eringen, who even in his later years continues to inspire young researchers in materials mechanics and continuum physics. The author also acknowledges the constructive comments of the anonymous reviewers.

Appendix A. Deformation measures and metric coefficients

The paper by Clayton et al. (2004) summarizes the derivation of deformation measures associated with the multiplicative decomposition of $\boldsymbol{F}$ and the existence of a non-Euclidean intermediate configuration $\overline{\mathscr{B}}$. It was shown that the covariant components of certain tensors in $\overline{\mathscr{B}}$ contain the covariant metric coefficients $\overline{G}_{\overline{K}\overline{L}}$. A short discussion proceeds here to put into context the formulation presented in this paper. It is reasonable to assume Cartesian coordinates for reference $\mathscr{B}_0$ and current $\mathscr{B}$ configurations for a continuum finite element implementation, but for now the metric coefficients g_{kl} and g^{kl} on $\mathscr{B}$ that appear in the formulation are left undefined, to be defined by a constitutive modeler later (and useful if implementing in a curved shell finite element method).

The deformation gradient, a second-order, two-point tensor $\boldsymbol{F}$ is written as (Marsden and Hughes, 1994)

$$\boldsymbol{F} = F^k_{\cdot K}\boldsymbol{g}_k \otimes \boldsymbol{G}^K \tag{106}$$

where $F^k_{\cdot K}$ are the mixed components associated with the covariant basis vectors $\boldsymbol{g}_k$ in $\mathscr{B}$ and contravariant basis vectors $\boldsymbol{G}^K$ in $\mathscr{B}_0$, and the dot $\cdot$ in front of K in the subscript denotes the order of indices, i.e. K is second and k is first. The multiplicative decomposition is then written as

$$\boldsymbol{F} = \boldsymbol{F}^e\boldsymbol{F}^p = \left[F^{ek}_{\cdot\overline{K}}\boldsymbol{g}_k \otimes \overline{\boldsymbol{G}}^{\overline{K}}\right]\left[F^{p\overline{J}}_{\cdot K}\overline{\boldsymbol{G}}_{\overline{J}} \otimes \boldsymbol{G}^K\right] = F^{ek}_{\cdot\overline{K}}F^{p\overline{K}}_{\cdot K}\boldsymbol{g}_k \otimes \boldsymbol{G}^K \tag{107}$$

where $\overline{\boldsymbol{G}}^{\overline{K}}$ are the contravariant basis vectors in $\overline{\mathscr{B}}$, and $\overline{\boldsymbol{G}}_{\overline{J}}$ the covariant basis vectors in $\overline{\mathscr{B}}$. Recall the transpose operation as (Marsden and Hughes, 1994)

$$\left(F^{eT}\right)^{\overline{K}}_{\cdot k} = \overline{G}^{\overline{K}\overline{L}}F^{el}_{\cdot\overline{L}}g_{kl} \tag{108}$$

Knowing $g_{kl} = \boldsymbol{g}_k\boldsymbol{g}_l$, it can be shown that the right elastic Cauchy–Green tensor is

$$\overline{\boldsymbol{C}}^e = \boldsymbol{F}^{eT}\boldsymbol{F}^e = F^{ek}_{\cdot\overline{K}}g_{kl}F^{el}_{\cdot\overline{L}}\overline{\boldsymbol{G}}^{\overline{K}} \otimes \overline{\boldsymbol{G}}^{\overline{L}} = \left[F^{ek}_{\cdot\overline{K}}\boldsymbol{g}_k\right]\left[F^{el}_{\cdot\overline{L}}\boldsymbol{g}_l\right]\overline{\boldsymbol{G}}^{\overline{K}} \otimes \overline{\boldsymbol{G}}^{\overline{L}} \tag{109}$$

Clayton et al. (2004) proposed the following definition for the covariant basis vectors in $\overline{\mathscr{B}}$ as

$$\overline{\boldsymbol{G}}_{\overline{K}} \overset{\text{def}}{=} F^{ek}_{\cdot\overline{K}}\boldsymbol{g}_k \tag{110}$$

such that

$$\overline{\boldsymbol{C}}^e = \left(\overline{\boldsymbol{G}}_{\overline{K}}\overline{\boldsymbol{G}}_{\overline{L}}\right)\overline{\boldsymbol{G}}^{\overline{K}} \otimes \overline{\boldsymbol{G}}^{\overline{L}} = \overline{G}_{\overline{K}\overline{L}}\overline{\boldsymbol{G}}^{\overline{K}} \otimes \overline{\boldsymbol{G}}^{\overline{L}} \tag{111}$$

which defines the covariant metric coefficients on $\overline{\mathscr{B}}$ as $\overline{G}_{\overline{K}\overline{L}} \overset{\text{def}}{=} \overline{C}^e_{\overline{K}\overline{L}} = F^{ek}_{\cdot\overline{K}}g_{kl}F^{el}_{\cdot\overline{L}}$. In summary, we have

$$\text{covariant metric in } \overline{\mathscr{B}}: \ \overline{G}_{\overline{K}\overline{L}} \overset{\text{def}}{=} \overline{C}^e_{\overline{K}\overline{L}} = F^{ek}_{\cdot\overline{K}}g_{kl}F^{el}_{\cdot\overline{L}} \tag{112}$$

$$\text{contravariant metric in } \overline{\mathscr{B}}: \ \overline{G}^{\overline{K}\overline{L}} \overset{\text{def}}{=} \left(\overline{C}^{e-1}\right)^{\overline{K}\overline{L}} = (F^{e-1})^{\overline{K}}_{\cdot k}g^{kl}(F^{e-1})^{\overline{L}}_{\cdot l} \tag{113}$$

where we used the orthogonality condition $\overline{G}_{\overline{K}\overline{L}}\overline{G}^{\overline{L}\overline{M}} = \delta^{\overline{M}}_{\overline{K}}$ to derive $\overline{G}^{\overline{K}\overline{L}}$ (Eringen, 1962). Normally, we assume the reference and current configurations are Cartesian for continuum finite element implementation (unless a general curvilinear finite element shell formulation is required). Another choice of covariant metric on $\overline{\mathscr{B}}$ would be to use the right elastic micro-deformation tensor as

$$\overline{\boldsymbol{C}}^{\chi,e} = \boldsymbol{\chi}^{eT}\boldsymbol{\chi}^e = \chi^{ek}_{\cdot\overline{K}}g_{kl}\chi^{el}_{\cdot\overline{L}}\overline{\boldsymbol{G}}^{\overline{K}} \otimes \overline{\boldsymbol{G}}^{\overline{L}} = \left[\chi^{ek}_{\cdot\overline{K}}\boldsymbol{g}_k\right]\left[\chi^{el}_{\cdot\overline{L}}\boldsymbol{g}_l\right]\overline{\boldsymbol{G}}^{\overline{K}} \otimes \overline{\boldsymbol{G}}^{\overline{L}} \tag{114}$$

where then $\overline{G}_{\overline{K}\overline{L}} \overset{\text{def}}{=} \overline{C}^{\chi,e}_{\overline{K}\overline{L}} = \chi^{ek}_{\cdot\overline{K}}g_{kl}\chi^{el}_{\cdot\overline{L}}$. The corresponding contravariant metric could likewise be reached through the orthogonality condition.

Remark 5. If elastic deformation measures in (39) or (119) are used, then metric coefficients on $\overline{\mathscr{B}}$ would need to be defined. The two choices of forms for plastic evolution equations in the paper outline all the required terms, regardless of choice of metric coefficients. But we note that for the elastic strain $\overline{E}^e_{\overline{K}\overline{L}}$ to not equal zero, then $\overline{G}_{\overline{K}\overline{L}} \neq \overline{C}^e_{\overline{K}\overline{L}}$, and thus the choice by Clayton et al. (2004) in (110) and (111) would lead to $\overline{E}^e_{\overline{K}\overline{L}} = 0$. Thus, for future finite element implementation, we will assume $\overline{\mathscr{B}}$ is Cartesian and $\overline{G}_{\overline{K}\overline{L}} = \delta_{\overline{K}\overline{L}}$.

Remark 6. It was mentioned in the introduction that the change in square of micro-element arc-lengths $(ds')^2 - \left(d\bar{s}'\right)^2$ should include only three unique elastic deformation measures (the two sets proposed by Eringen (1999) and considered in this paper for finite strain elastoplasticity). Here, we write directly

$$(ds')^2 = d\boldsymbol{x}'d\boldsymbol{x}' = dx'^k g_{kl}dx'^l \tag{115}$$

where

$$dx'^k = F^{ek}_{\cdot\overline{K}}d\overline{X}^{\overline{K}} + \chi^{ek}_{\cdot\overline{K}\overline{L}}\Xi^{\overline{K}}d\overline{X}^{\overline{L}} + \chi^{ek}_{\cdot\overline{K}}\chi^{p\overline{K}}_{\cdot K\overline{L}}\Xi^K d\overline{X}^{\overline{L}} + \chi^{ek}_{\cdot\overline{K}}d\Xi^{\overline{K}} \tag{116}$$

Then

$$
\begin{aligned}
(ds')^2 = &\left[\overline{C}^e_{\overline{K}\overline{L}} + 2\mathrm{sym}\left(\overline{\Gamma}^e_{\overline{K}\overline{B}\overline{L}}\right)\overline{\Xi}^{\overline{B}} + \overline{\Gamma}^e_{\overline{D}\overline{A}\overline{K}}\left(\overline{C}^{e-1}\right)^{\overline{D}\,\overline{M}}\overline{\Gamma}^e_{\overline{M}\overline{B}\overline{L}}\overline{\Xi}^{\overline{A}}\overline{\Xi}^{\overline{B}}\right.\\
&+2\mathrm{sym}\left(\overline{\Psi}^e_{\overline{B}\overline{E}}\left(\overline{C}^{e-1}\right)^{\overline{B}\,\overline{C}}\overline{\Gamma}^e_{\overline{C}\overline{A}\overline{K}}\chi^{p\overline{E}}_{\cdot E,\overline{L}}\right)\overline{\Xi}^{\overline{A}}\Xi^{E}\\
&\left.+\overline{\Psi}^e_{\overline{A}\overline{D}}\left(\overline{C}^{e-1}\right)^{\overline{A}\,\overline{B}}\overline{\Psi}^e_{\overline{B}\overline{E}}\chi^{p\overline{D}}_{\cdot D,\overline{K}}\chi^{p\overline{E}}_{\cdot E,\overline{L}}\Xi^{D}\Xi^{E} + 2\mathrm{sym}\left(\overline{\Psi}^e_{\overline{K}\overline{E}}\chi^{p\overline{E}}_{\cdot E,\overline{L}}\right)\Xi^{E}\right]d\overline{X}^{\overline{K}}d\overline{X}^{\overline{L}}\\
&+2\left[\overline{\Psi}^e_{\overline{K}\overline{L}} + \overline{\Psi}^e_{\overline{B}\overline{L}}\left(\overline{C}^{e-1}\right)^{\overline{B}\,\overline{C}}\overline{\Gamma}^e_{\overline{C}\overline{A}\overline{K}}\overline{\Xi}^{\overline{A}}\right.\\
&\left.+\overline{\Psi}^e_{\overline{A}\overline{L}}\left(\overline{C}^{e-1}\right)^{\overline{A}\,\overline{B}}\overline{\Psi}^e_{\overline{B}\overline{D}}\chi^{p\overline{D}}_{\cdot D,\overline{K}}\Xi^{D}\right]d\overline{X}^{\overline{K}}d\overline{\Xi}^{\overline{L}}\\
&+\left[\overline{\Psi}^e_{\overline{A}\overline{K}}\left(\overline{C}^{e-1}\right)^{\overline{A}\,\overline{B}}\overline{\Psi}^e_{\overline{B}\overline{L}}\right]d\overline{\Xi}^{\overline{K}}d\overline{\Xi}^{\overline{L}}
\end{aligned}
\tag{117}
$$

and

$$
\left(d\overline{S}'\right)^2 = \overline{G}_{\overline{K}\overline{L}}\left(d\overline{X}^{\overline{K}}d\overline{X}^{\overline{L}} + 2d\overline{X}^{\overline{K}}d\overline{\Xi}^{\overline{L}} + d\overline{\Xi}^{\overline{K}}d\overline{\Xi}^{\overline{L}}\right) \tag{118}
$$

It can be seen that the first set in (39) appears exclusively as elastic deformation in (117); there are also some plastic terms, which do not appear in (1.5.8) in Eringen (1999). Eq. (117) could likewise be expressed in terms of the elastic set in (119). But one or the other set is unique, as outlined by Eringen (1999) for micromorphic elasticity, here put into context for finite strain micromorphic elastoplasticity.

Appendix B. Another set of elastic deformation measures

Here, another set of elastic deformation measures, (1.5.11) in Eringen (1999), are considered in their covariant components as

$$
\begin{aligned}
&\overline{C}^{\chi,e}_{\overline{K}\overline{L}} = \chi^{ek}_{\cdot\overline{K}}g_{kl}\chi^{el}_{\cdot\overline{L}}, \quad \overline{\Upsilon}^e_{\overline{K}\overline{L}} = \overline{G}_{\overline{A}\overline{L}}(\chi^{e-1})^{\overline{A}}_{\cdot a}F^{ea}_{\cdot\overline{K}},\\
&\overline{\Pi}^e_{\overline{K}\overline{L}\overline{M}} = \overline{G}_{\overline{A}\overline{K}}(\chi^{e-1})^{\overline{A}}_{\cdot a}\chi^{ea}_{\cdot\overline{L},\overline{M}}
\end{aligned}
\tag{119}
$$

Thus, the Helmholtz free energy function is written as

$$
\bar{\rho}\bar{\psi}\left(\overline{C}^{\chi,e}_{\overline{K}\overline{L}}, \overline{\Upsilon}^e_{\overline{K}\overline{L}}, \overline{\Pi}^e_{\overline{K}\overline{L}\overline{M}}, \overline{Z}^{\overline{K}}, \overline{Z}^{\chi\overline{K}}, \overline{Z}^{\overline{K}}_{\cdot\overline{L}}, \theta\right) \tag{120}
$$

and the constitutive equations for stress result from (34)–(36) as

$$
\overline{S}^{\overline{K}\overline{L}} = \frac{\partial\left(\bar{\rho}\bar{\psi}\right)}{\partial\overline{\Upsilon}^e_{\overline{K}\overline{B}}}\overline{G}_{\overline{B}\overline{C}}(\chi^{e-1})^{\overline{C}}_{\cdot k}g^{kl}(F^{e-1})^{\overline{L}}_{\cdot l} \tag{121}
$$

$$
\overline{\Sigma}^{\overline{K}\overline{L}} = 2\left(\overline{\Upsilon}^{e-1}\right)^{\cdot\overline{K}}_{\overline{A}}\frac{\partial\left(\bar{\rho}\bar{\psi}\right)}{\partial\overline{C}^{\chi,e}_{\overline{A}\overline{B}}}\left(\overline{\Upsilon}^{e-1}\right)^{\cdot\overline{L}}_{\overline{B}} \tag{122}
$$

$$
\overline{M}^{\overline{K}\overline{L}\overline{M}} = \frac{\partial\left(\bar{\rho}\bar{\psi}\right)}{\partial\overline{\Pi}^e_{\overline{I}\overline{M}\overline{K}}}\overline{G}_{\overline{I}\overline{B}}(\chi^{e-1})^{\overline{B}}_{\cdot k}g^{kl}(F^{e-1})^{\overline{L}}_{\cdot l} \tag{123}
$$

where $\left(\overline{\Upsilon}^{e-1}\right)^{\cdot\overline{K}}_{\overline{A}} = (F^{e-1})^{\overline{K}}_{\cdot k}\chi^{ek}_{\cdot\overline{A}}$. These stress equations take a somewhat simpler form than in (41)–(43), but now the metric coefficients appear directly. Thus, it becomes a choice of the modeler how the specific constitutive form of the elastic part of the Helmholtz free energy function is written, i.e. in terms of (40) or (120). Eringen (1999) advocated the use of (120) for micromorphic elasticity, whereas Suhubi and Eringen (1964) used (40). We use (40) in Section 7.

Appendix C. Derivation of $\boldsymbol{F}'$

The formulation of (5) is presented in this appendix, and we will use direct notation. To start, we recognize that

$$
\boldsymbol{F}' = \frac{\partial\boldsymbol{x}'}{\partial\boldsymbol{X}'} = \frac{\partial\boldsymbol{x}'}{\partial\boldsymbol{X}}\frac{\partial\boldsymbol{X}}{\partial\boldsymbol{X}'} \tag{124}
$$

where

$$
\frac{\partial\boldsymbol{x}'}{\partial\boldsymbol{X}} = \boldsymbol{F} + \frac{\partial\boldsymbol{\chi}}{\partial\boldsymbol{X}}\boldsymbol{\Xi} + \boldsymbol{\chi}\frac{\partial\boldsymbol{\Xi}}{\partial\boldsymbol{X}} \tag{125}
$$

and

$$
\frac{\partial\boldsymbol{X}}{\partial\boldsymbol{X}'} = \mathbf{1} - \frac{\partial\boldsymbol{\Xi}}{\partial\boldsymbol{X}'} \tag{126}
$$

It is possible to show that $\partial\boldsymbol{\Xi}/\partial\boldsymbol{X}' \approx \partial\boldsymbol{\Xi}/\partial\boldsymbol{X}$, starting with

$$
\frac{\partial\boldsymbol{\Xi}}{\partial\boldsymbol{X}'} = \frac{\partial\boldsymbol{\Xi}}{\partial\boldsymbol{X}}\frac{\partial\boldsymbol{X}}{\partial\boldsymbol{X}'} \tag{127}
$$

which using (126) leads to

$$
\frac{\partial\boldsymbol{\Xi}}{\partial\boldsymbol{X}'} = \left(\mathbf{1} + \frac{\partial\boldsymbol{\Xi}}{\partial\boldsymbol{X}}\right)^{-1}\frac{\partial\boldsymbol{\Xi}}{\partial\boldsymbol{X}} \tag{128}
$$

If we assume the gradient of microstructure is small across a material $\|\partial\boldsymbol{\Xi}/\partial\boldsymbol{X}\| \ll 1$ (for the region of interest where the micromorphic continuum model is used), then

$$
\left(\mathbf{1} + \frac{\partial\boldsymbol{\Xi}}{\partial\boldsymbol{X}}\right)^{-1} \approx \mathbf{1} - \frac{\partial\boldsymbol{\Xi}}{\partial\boldsymbol{X}} \tag{129}
$$

where then

$$
\frac{\partial\boldsymbol{\Xi}}{\partial\boldsymbol{X}'} = \left(\mathbf{1} - \frac{\partial\boldsymbol{\Xi}}{\partial\boldsymbol{X}}\right)\frac{\partial\boldsymbol{\Xi}}{\partial\boldsymbol{X}} \approx \frac{\partial\boldsymbol{\Xi}}{\partial\boldsymbol{X}} \tag{130}
$$

The expression for $\boldsymbol{F}'$ then results as in (5).

References

Bilby, B., Bullough, R., Smith, E., 1955. Continuous distributions of dislocations: a new application of the methods of non-Riemannian geometry. Proc. Roy. Soc. Lond. Ser. A 231, 263–273.

Birgisson, B., Soranakom, C., Napier, J., Roque, R., 2004. Microstructure and fracture in asphalt mixtures using a boundary element approach. J. Mater. Civil Eng. 16 (2), 116–121.

Caballero, A., Lopez, C., Carol, I., 2006. 3D Meso-structural analysis of concrete specimens under uniaxial tension. Comput. Methods Appl. Mech. Eng. 195 (52), 7182–7195.

Cermelli, P., Gurtin, M.E., 2001. On the characterization of geometrically necessary dislocations in finite plasticity. J. Mech. Phys. Solids 49, 1539–1568.

Chevalier, Y., Pahr, D., Allmer, H., Charlebois, M., Zysset, P., 2007. Validation of a voxel-based fe method for prediction of the uniaxial apparent modulus of human trabecular bone using macroscopic mechanical tests and nanoindentation. J. Biomech. 40 (15), 3333–3340.

Clayton, J., Bammann, D., McDowell, D., 2004. Anholonomic configuration spaces and metric tensors in finite elastoplasticity. Int. J. Non. Linear Mech. 39 (6), 1039–1049.

Clayton, J., Bammann, D., McDowell, D., 2005. A geometric framework for the kinematics of crystals with defects. Philos. Mag. 85 (33–35), 3983–4010.

Clayton, J., McDowell, D., Bammann, D., 2006. Modeling dislocations and disclinations with finite micropolar elastoplasticity. Int. J. Plasticity 22 (2), 210–256.

Coleman, B.D., Noll, W., 1963. The thermodynamics of elastic materials with heat conduction and viscosity. Arch. Ration. Mech. Anal. 13, 167–178.

Dai, Q., Sadd, M., Parameswaran, V., Shukla, A., 2005. Prediction of damage behaviors in asphalt materials using a micromechanical finite-element model and image analysis. J. Eng. Mech. 131 (7), 668–677.

Desai, C., Siriwardane, H., 1984. Constitutive Laws for Engineering Materials: With Emphasis on Geologic Materials. Prentice-Hall, Englewood Cliffs, NJ.

Eringen, A., 1962. Nonlinear Theory of Continuous Media, first ed. McGraw-Hill, New York.

Eringen, A., 1968. Theory of micropolar elasticity. In: Liebowitz, H. (Ed.), Fracture: An Advanced Treatise, vol. 2. Academic Press, New York, pp. 622–729.

Eringen, A., 1999. Microcontinuum Field Theories I: Foundations and Solids. Springer, Berlin.

Eringen, A., Suhubi, E., 1964. Nonlinear theory of simple micro-elastic solids – I. Int. J. Eng. Sci. 2 (2), 189–203.

Fish, J., 2006. Bridging the scales in nano engineering and science. J. Nanoparticle Res. 8 (5), 577–594.

Forest, S., Sievert, R., 2003. Elastoviscoplastic constitutive frameworks for generalized continua. Acta Mech. 160 (1–2), 71–111.

Forest, S., Sievert, R., 2006. Nonlinear microstrain theories. Int. J. Solids Struct. 43 (24), 7224–7245.

Formica, G., Sansalone, V., Casciaro, R., 2002. A mixed solution strategy for the nonlinear analysis of brick masonry walls. Comput. Methods Appl. Mech. Eng. 191 (51–52), 5847–5876.

Germain, P., 1973. The method of virtual power in the mechanics of continuous media. II. Microstructure. SIAM J. Appl. Math. 25 (3), 556–575.

Hill, R., 1950. The Mathematical Theory of Plasticity. Clarendon Press, Oxford.

Holzapfel, G.A., 2000. Nonlinear Solid Mechanics: A Continuum Approach for Engineering. Wiley, New York.

Kondo, K., 1952. On the geometrical and physical foundations of the theory of yielding. In: Proceedings of the Second Japan National Congress for Applied Mechanics, pp. 41–47.
Kröner, E., 1960. Allgemeine kontinuumstheorie der versetzungen and eigenspannungen. Arch. Ration. Mech. Anal. 4, 273–334.
Lee, E., 1969. Elastic–plastic deformation at finite strains. J. Appl. Mech. 36, 1–6.
Lee, J., Chen, Y., 2003. Constitutive relations of micromorphic thermoplasticity. Int. J. Eng. Sci. 41 (3–5), 387–399.
Lee, E.H., Liu, D.T., 1967. Finite-strain elastic–plastic theory with application to plane-wave analysis. J. Appl. Phys. 38, 19–27.
Lee, J., Chen, Y., Zeng, X., Eskandarian, A., Oskard, M., 2007. Modeling and simulation of osteoporosis and fracture of trabecular bone by meshless method. Int. J. Eng. Sci. 45 (2–8), 329–338.
Lubliner, J., 1990. Plasticity Theory. Macmillan, New York.
Maiti, S., Rangaswamy, K., Geubelle, P., 2005. Mesoscale analysis of dynamic fragmentation of ceramics under tension. Acta Mater. 53 (3), 823–834.
Mandel, J., 1974. Thermodynamics and plasticity. In: Delgado, J.J. et al. (Eds.), Foundations of Continuum Thermodynamics. Macmillan, New York, pp. 283–304.
Marsden, J., Hughes, T., 1994. Mathematical Foundations of Elasticity. Dover, New York.
Maugin, G., 1992. The Thermomechanics of Plasticity and Fracture. Cambridge University Press, Cambridge.
Mindlin, R., 1964. Microstructure in linear elasticity. Arch. Ration. Mech. Anal. 16, 51–78.
Molinari, J., Warner, D., 2006. Micromechanical finite element modeling of compressive fracture in confined alumina ceramic. Acta Mater. 54 (19), 5135–5145.
Moran, B., Ortiz, M., Shih, C., 1990. Formulation of implicit finite-element methods for multiplicative finite deformation plasticity. Int. J. Numer. Methods Eng. 29 (3), 483–514.
Morris, J., Rubin, M., Block, G., Bonner, M., 2006. Simulations of fracture and fragmentation of geologic materials using combined FEM/DEM analysis. Int. J. Impact Eng. 33 (1–12), 463–473.
Nemat-Nasser, S., 2004. Plasticity: A Treatise on the Finite Deformation of Heterogeneous Inelastic Materials. Cambridge University Press, Cambridge.
Nezami, E., Hashash, Y., Zhao, D., Ghaboussi, J., 2007. Simulation of front end loader bucket–soil interaction using discrete element method. Int. J. Numer. Anal. Methods Geomech. 31 (9), 1147–1162.
Regueiro, R., 2009. Finite strain micromorphic pressure-sensitive plasticity. J. Eng. Mech. 135, 178–191.
Regueiro, R., Dixit, P., Garikipati, K., 2007. On standard and vector finite element analysis of a strict anti-plane shear plasticity model with elastic curvature. Comput. Methods Appl. Mech. Eng. 196, 2692–2712.
Sadowski, T., Postek, E., Denis, C., 2007. Stress distribution due to discontinuities in polycrystalline ceramics containing metallic inter-granular layers. Comput. Mater. Sci. 39 (1), 230–236.
Sansour, C., 1998. Unified concept of elastic–viscoplastic cosserat and micromorphic continua. J. Phys. IV 8 (8), 341–348.
Simo, J.C., 1998. Numerical analysis and simulation of plasticity. In: Ciarlet, P., Lions, J. (Eds.), Handbook of Numerical Analysis. Elsevier Science, Amsterdam.
Simo, J.C., Hughes, T.J.R., 1998. Computational Inelasticity. Prentice-Hall, New York.
Suhubi, E., Eringen, A., 1964. Nonlinear theory of simple micro-elastic solids – II. Int. J. Eng. Sci. 2 (2), 389–404.
Vernerey, F., Liu, W., Moran, B., 2007. Multi-scale micromorphic theory for hierarchical materials. J. Mech. Phys. Solids 55 (12), 2603–2651.
Vogler, T., Clayton, J., 2008. Heterogeneous deformation and spall of an extruded tungsten alloy: plate impact experiments and crystal plasticity modeling. J. Mech. Phys. Solids 56 (2), 297–335.